Synthesis and Supramolecular Assembly of Highly Planar Amphiphilic Porphyrin Complexes

Masafumi Oda

DOCTOR OF PHILOSOPHY

Department of Structural Molecular Science

School of Physical Sciences

The Graduate University for Advanced Studies

2009

Contents

Chapter 1.

General Introduction

1-1 Supramolecular Integration of Porphyrin and its Derivatives

The supramolecular integration of porphyrin and the derivatives has obtained great attention because of the relevance to the natural photosynthetic systems, where a large number of chromophores are spatially aligned and the mutual distances are completely controlled (Figure 1-1).[1] For example, light-harvesting antenna in photosynthetic purple bacteria have been extensively investigated because of interest in the structures and the photophysical properties. At the membrane of purple bacteria, bacterio-chlorophylls (BChl) are arranged into cyclic structures, so-called LH1 and LH2 (Figure 1-2), where light energy absorbed is transferred efficiently from the smaller LH2 ring to the larger LH1 and finally delivered to the reaction center (RC). Green photosynthetic bacteria utilize chlorosomes as the main light harvesting system,[2] which includes the most efficient antenna known so far and a lamellar organization of a large number of pigments (BChl) has been proposed to the antenna by Tuma *et al*. in 2004 (Figure 1-3).[2c]

These studies mentioned above have revealed the important correlation between molecular arrangements of chromophores and the physical properties, which motivated us to investigate the potentials of porphyrin aggregates for useful applications.

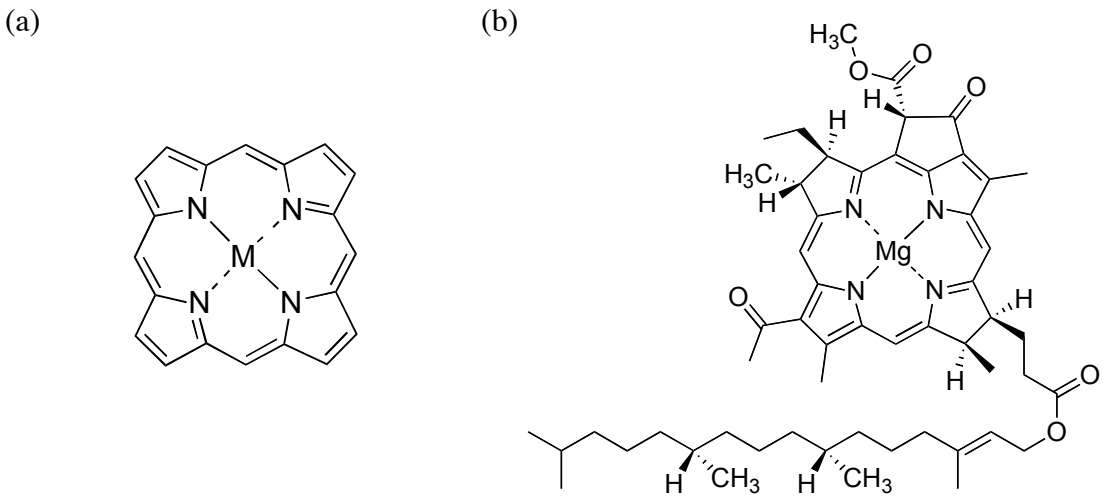

Figure 1-1. The structure of (a) porphyrin skeleton and (b) BChl *a*.

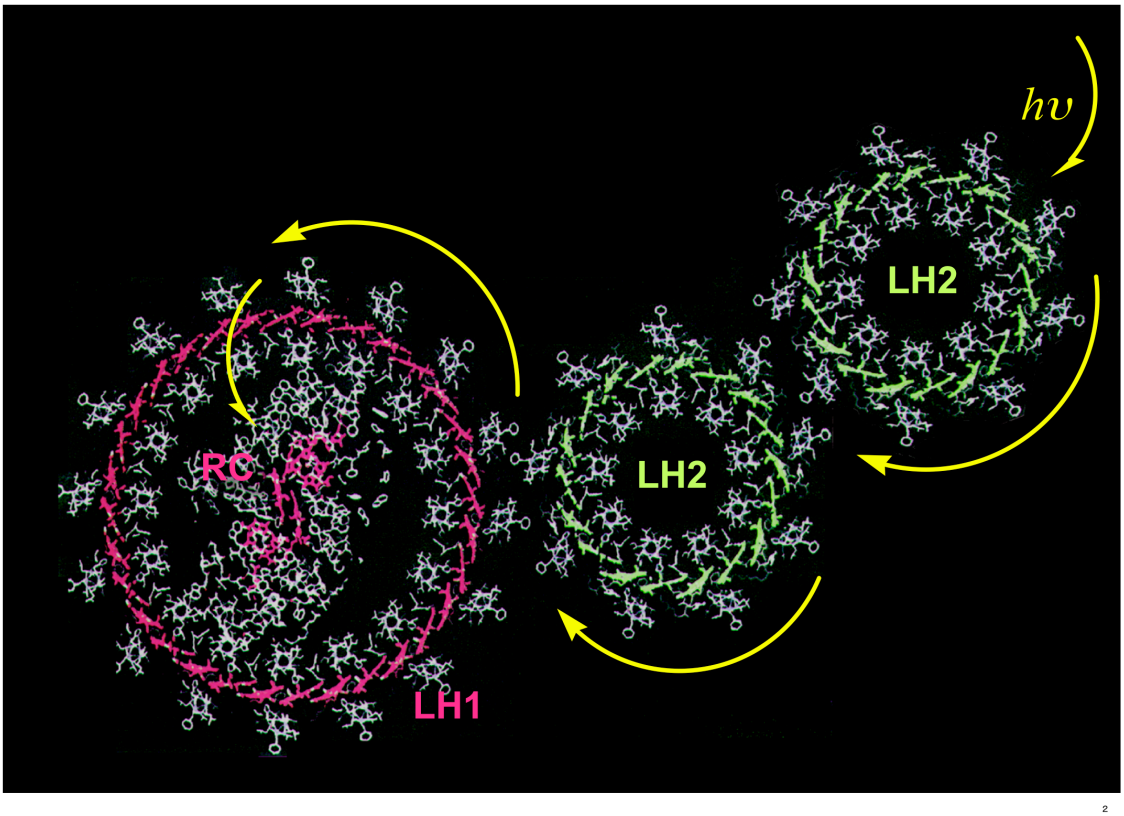

Figure 1-2. Arrangement of pigment–protein complexes at the membrane of purple bacteria. All the BChls are in green or red.

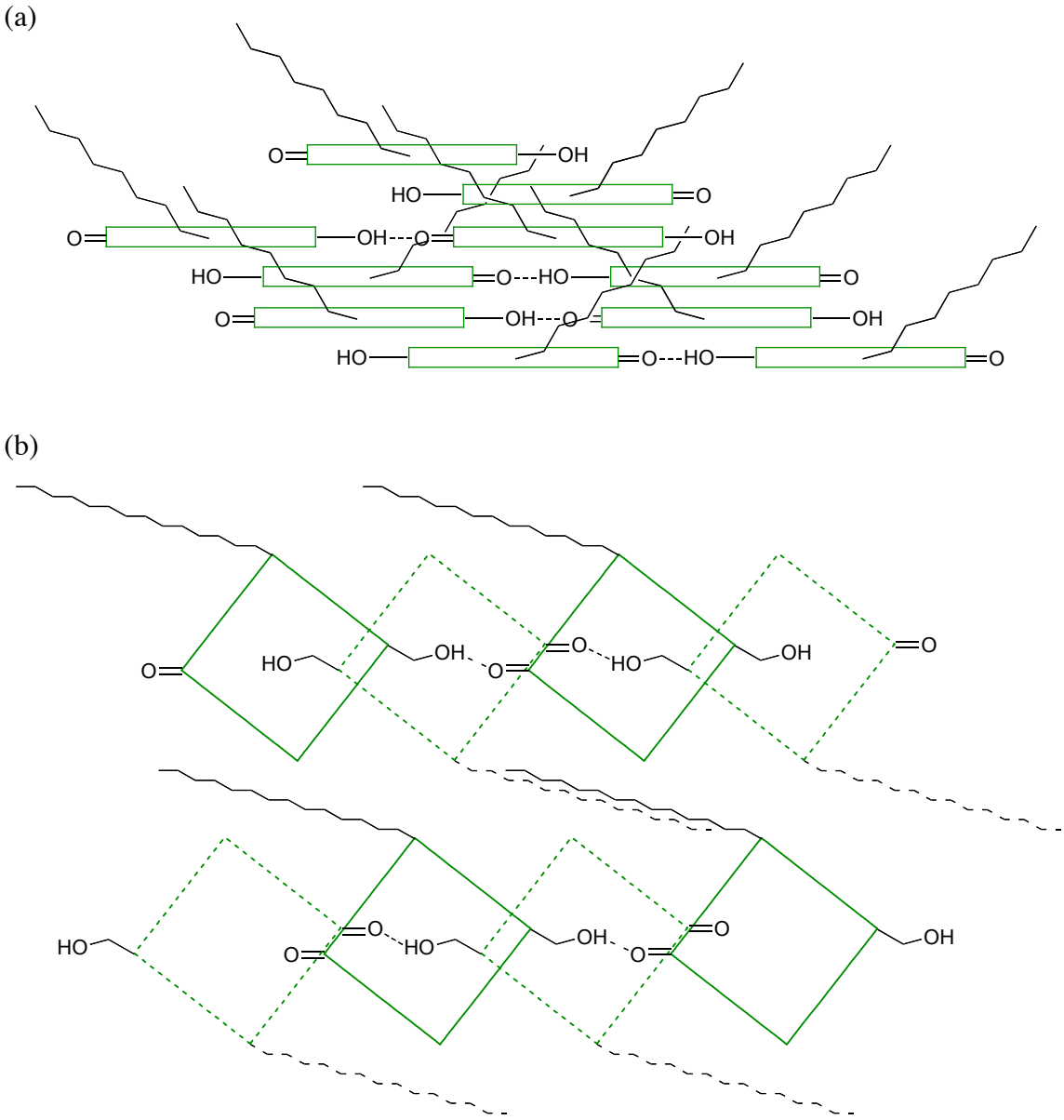

Figure 1-3. Schematic model of the BChl aggregates in the chlorosome. (a) Model of one plane of BChl aggregate with antiparallel pigment configuration. (b) Top view of chlorin (*green*) planes (antiparallel configuration) associated via interdigitated esterifying alcohol tails (*black*). An underlying layer of BChl molecules is shown dotted.

In order to obtain well-defined porphyrin aggregates,[3] many types of the molecule have been designed and synthesized for these years. Not only covalent bonding[4] but metal coordination,[5] hydrogen-bonding[6] and van der Waals interaction[7] have been utilized and the obtained integrated structures have been employed for application in the fields of sensors, field-effect transistors and photovoltaic cells, *etc*.[3b,8]

Construction of porphyrin-based macrorings as model compounds of natural light-harvesting antenna has been a challenging target to find a solution of their excellent energy transfer properties. Wheel-like dendritic molecules appended with multiple porphyrin units have been synthesized and the electron transfer reaction between fullerene units as an accepter has been studied by Jiang and Aida *et al*. (Figure 1-4(a)).[4d] Kobuke *et al*. have developed metal-coordination methodology for construction of macrorings with two imidazolylporphyrinatozinc combined together through appropriate linker (Figure 1-4(b)).[5e,f] Meanwhile, lamellar organization of porphyrins like chlorosomes has also been researched widely and this type of self-assembly of porphyrins requires non-covalent interactions between the side groups and π-π stacking between porphyrin cores. Huijser *et al*. have studied relationship between self-assembled structures and the transportation ability of excitons for porphyrin derivatives, and demonstrated the importance of ordered structure leading to efficient interstack exciton transport (Figure 1-5(a)).[5a] Shinkai *et al*. have reported that hydrogen-bonding porphyrins appended by amide-, urea- or sugar-group afforded different ordered structures such as sheets, fibers or helixes, *etc*. which are controlled by the manner of the intermolecular hydrogen bonding (Figure 1-5(b)).[6]

Development of controlled molecular organization is indispensable in relation to bottom-up methodology for the production of next-generation nanomaterials.

Porphyrin is one of good building blocks for that kind of studies because of its abundant past studies and the feasibility of various molecular designs.

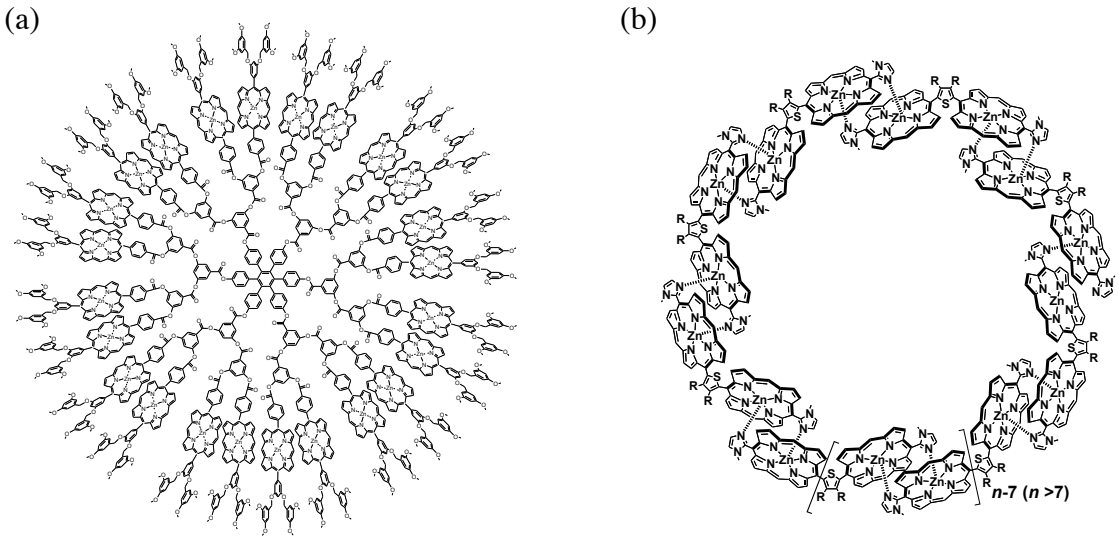

Figure 1-4. The porphyrin macrorings synthesized (a) from a dendritic scaffold and (b) by mutual coordination.

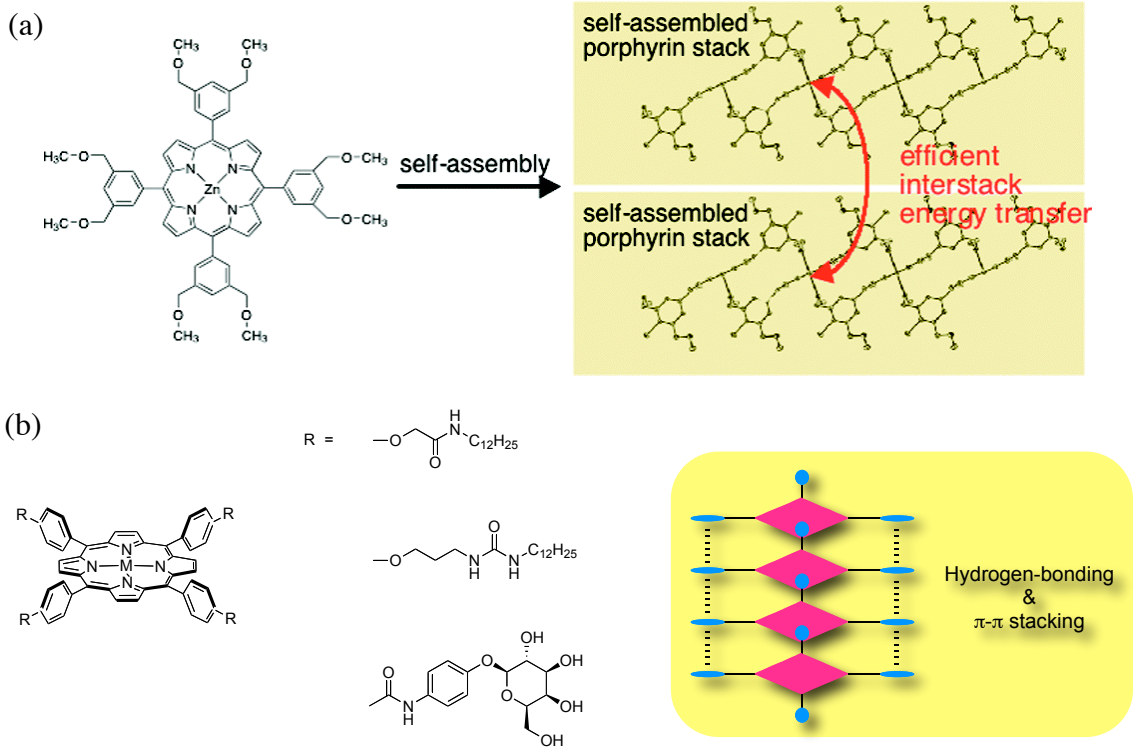

Figure 1-5. Lamellar organization of porphyrins assisted by (a) metal coordination and (b) hydrogen-bonding. (Figure 1-5(a) was replaced from the literature.[5a])

1-2 Amphiphilic Motives with Rigid π-Cores

Amphiphiles are quite known to form well-ordered aggregates spontaneously and this ability has been used for cell walls or surface-active agents, *etc*. Recently, amphiphilic motives with rigid π-cores have been well employed to obtain excellent optoelectronic properties associated with the characteristic nanostructures.[9] For example, one of the most famous works of that kind of study is self-assembled amphiphilic hexabenzocoronene nanotubes with photochemical properties by Aida *et al* (Figure 1-6(a)).[9b,c] Tashiro and Aida *et al*. have reported interesting liquid crystalline properties of an amphiphilic fully-fused porphyrin dimer, affiliated with the electric conductivity (Figure 1-6 (b)).[9h] Ishizuka and Jiang *et al*. have also investigated the semiconducting conductivity and intermolecular magnetic interaction of a one-dimensional molecular wire consisted of amphiphilic dinuclear schiff-base complexes which show a remarkable H-aggregated state in a polar solvent. Because of the high planarity of these complexes, they can be integrated densely packed nanostructures leading to unique characteristics (Figure 1-6 (c)).[9i]

Because of the potentials of this type of molecules for nanoscience, amphiphilic π-conjugated systems are worth examining not only for fundamental studies but also for future application in industries.

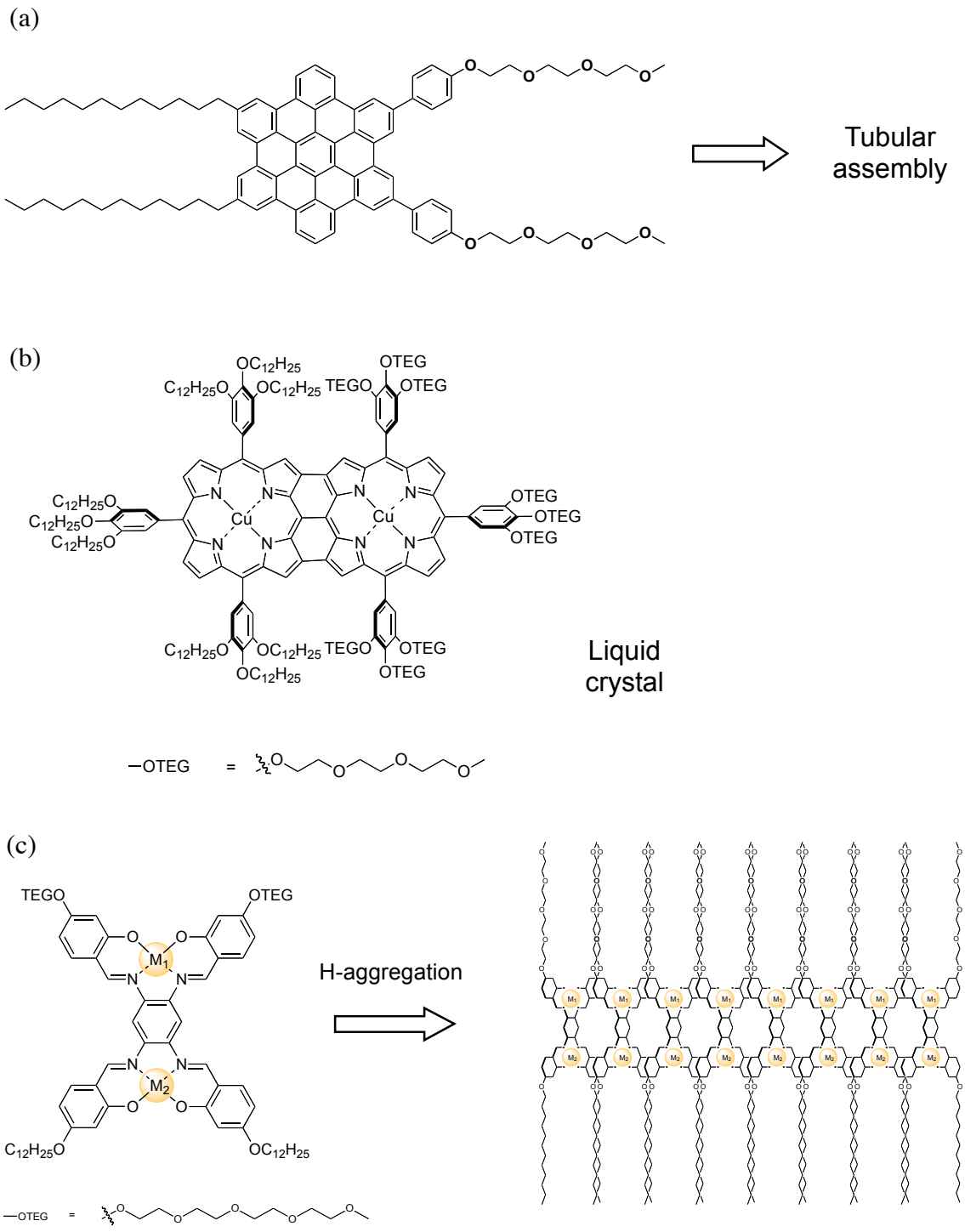

Figure 1-6. Amphiphilic motives with rigid π-cores; the core parts are (a) hexabenzocoronene, (b) fully-fused triphenylporphyrin dimer and (c) planar dinuclear schiff-base complexes.

1-3 Design and Synthetic Strategy of a Porphyrin in order to Accomplish Densely Packed Nanostructures

Amphiphilic porphyrin complexes are quite interesting synthetic target because they can be integrated well-ordered supramolecules and they are also useful to reveal the relationship between the spatial arrangement and the physical properties of the molecules.

1-3-1 meso-Aryl Type vs. β-Alkyl Type Porphyrins

Generally, synthetic porphyrins are classified into two species; one is called "*meso*-aryl type" and the other is "*β*-alkyl type" (Figure 1-7). *Meso*-aryl porphyrin is used more frequently for researches in recent years than *β*-alkylporphyrin because it can be synthesized with shorter reaction steps and thus more complicated modification is also possible. This porphyrin, however, includes larger steric bulkiness caused by the aromatic rings at the *meso*-positions. On the other hand, *β*-alkylporphyrin is difficult to be synthesized, especially for asymmetrically substituted ones, but it has no bulky groups at the periphery. Therefore, porphyrin molecule is highly planar. In this dissertation, metal complexes of *β*-alkyl type porphyrin are employed in order to accomplish densely packed nanostructures and hence they may induce strong intermolecular interactions between the metal centers.

(a) (b)

Figure 1-7. Conventional pophyrins; (a) *meso*-aryl type and (b) *β*-alkyl type pophyrin.

1-3-2 Design of Amphiphilic β-Alkylporphyrin Complexes

Here, a novel amphiphilic *β*-alkylporphyrin complex **1**-M is designed, which tethered alkyl and triethyleneglycol (TEG) chains as hydrophobic and hydrophilic components, respectively (Figure 1-8). For this porphyrin **1**-M, Israelachvili's critical packing parameter (P_c) is calculated to be less than 1/3, implying that spherical micelles should be favorably formed in polar solvents.[9e,10] From the optimized structure at AM1 level, compound **1**-M is much planar and less bulky to be assembled in densely packed supramolecules (Figure 1-9). In addition, the empty *β*-positions may support high reactivity of the *meso*-positions for substitution reactions with functional groups, and furthermore it can be applied to *meso-meso*-linked porphyrin arrays.[11]

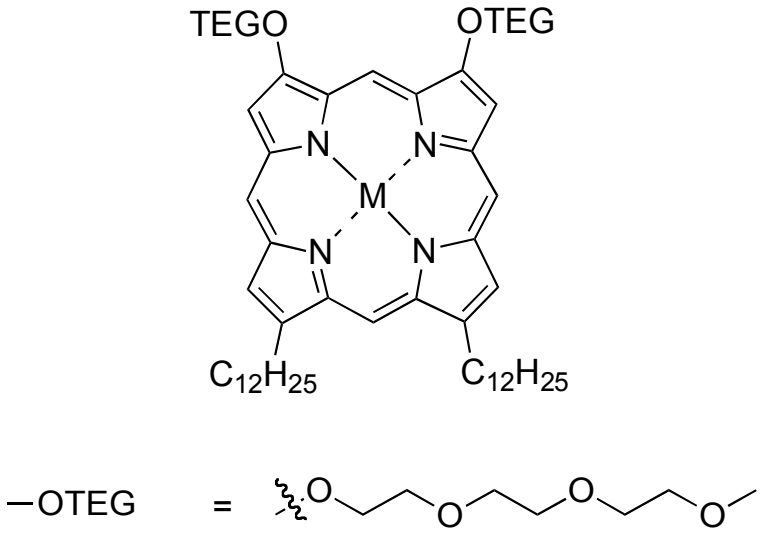

Figure 1-8. Amphiphilic β-alkylporphyrin complex **1**-M.

(a)

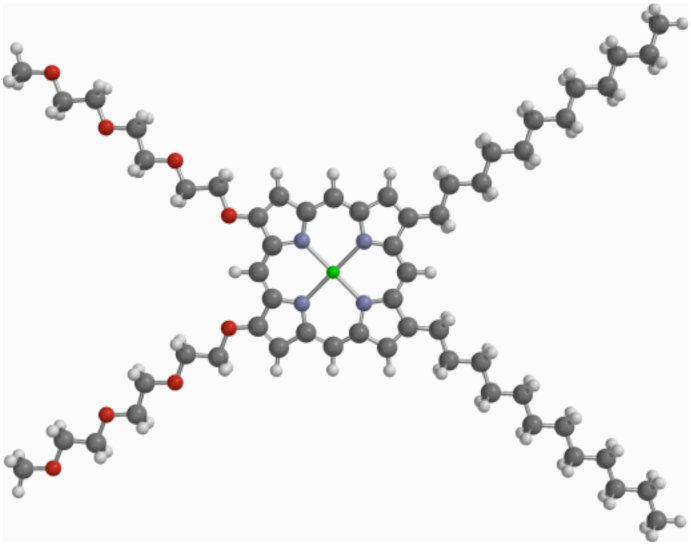

(b)

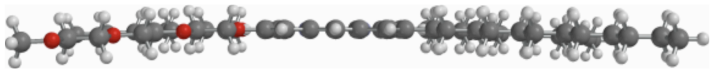

Figure 1-9. Optimized structure of **1**-Zn at AM1 level. (a) Top and (b) side views.

1-3-3 Retrosynthetic Analysis of the Target Porphyrin

To obtain the amphiphilic *β*-alkylporphyrin complexes **1**-M, the synthetic route have been analyzed retrosynthetically (Scheme 1-1). The target porphyrin **1**-M can be synthesized by the condensation reaction of TEG-tethered and alkyl-tethered dipyrromethanes. These can be obtained from 4-position substituted ethyl pyrrole-2(and 3)-carboxylate by the dimerization and the decarboxylation. Consequently, the first key subjects are syntheses of these pyrroles.

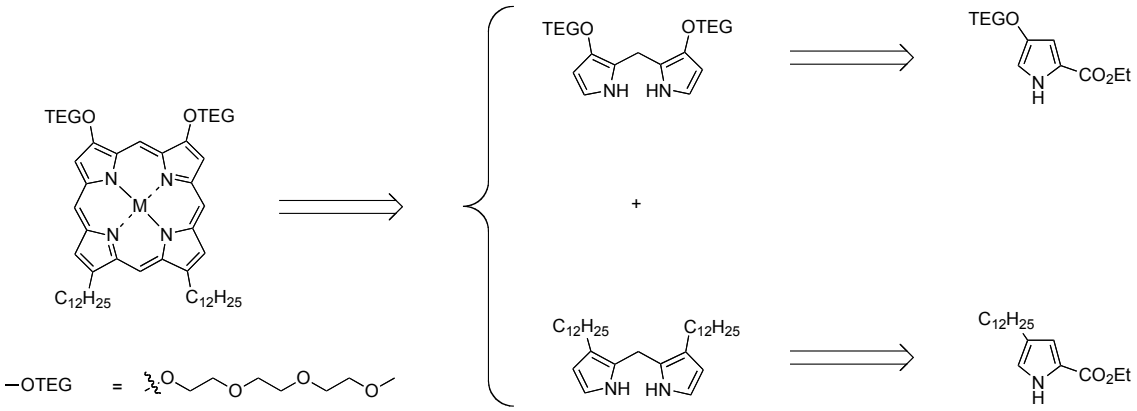

Scheme 1-1. Retrosynthetic analysis for target porphyrin **1**-M.

1-4 References

1. (a) McDermott, G.; Prince, S. M.; Freer, A. A.; Hawthornthwaite-Lawless, A. M.; Papiz, M. Z.; Cogdell, R. J.; Isaacs, N. W. *Nature,* **1995**, *374*, 517-521. (b) Hu, X.; Damjanovic, A.; Ritz, T.; Schulten, K. *Proc. Natl. Acad. Sci. USA*, **1998**, *95*, 5935-5941. (c) Roszak, A. W.; Howard, T. D.; Southall, J.; Gardiner, A. T.; Law, C. J.; Isaacs, N. W.; Cogdell, R. J. *Science*, **2003**, *302*, 1969-1972.
2. (a) Staehelin, L. A.; Golecki, J. R.; Fuller, R. C.; Drews, G. *Arch. Microbiol.* **1978**, *119*, 269-277. (b) Frigaard, N. U.; Bryant, D. A. *Arch. Microbiol.* **2004**, *182*, 265-276. (c) Psencik, J.; Ikonen, T. P.; Laurinmaki, P.; Merckel, M. C.; Butcher, S. J.; Serimaa, R. E.; Tuma, R. *Biophys. J.* **2004**, *87*, 1165-1172.
3. Recent reviews: (a) Balaban, T. S. *Acc. Chem. Res.* **2005**, *38*, 612-623. (b) Elemans, J. A. A. W.; van Hameren, R.; Nolte, R. J. M.; Rowan, A. E. *Adv. Mater.* **2006**, *18*, 1251-1266.
4. (a) Aratani, N.; Osuka, A.; Kim, Y. H.; Jeong, D. H.; Kim, D. *Angew. Chem. Int. Ed.* **2000**, *39*, 1458-1462. (b) Tsuda, A.; Osuka, A. *Science*, **2001**, *293*, 79-82. (c) Duncan, T. V.; Susumu, K.; Sinks, L. E.; Therien, M. J. *J. Am. Chem. Soc.* **2006**, *128*, 9000-9001. (d) Li, W.-S.; Kim, K. S.; Jiang, D.-L.; Tanaka, H.; Kawai, T.; Kwon, J. H.; Kim, D.; Aida, T. *J. Am. Chem. Soc.* **2006**, *128*, 10527-10532.
5. (a) Huijser, A.; Suijkerbuijk, B. M. J. M.; Gebbink, R. J. M. K.; Savenije, T. J.; Siebbeles, L. D. A. *J. Am. Chem. Soc.* **2008**, *130*, 2485-2492. (b) Lee, S. J.; Mulfort, K. L.; Zuo, X.; Goshe, A. J.; Wesson, P. J.; Nguyen, S. T.; Hupp, J. T.; Tiede, D. M. *J. Am. Chem. Soc.* **2008**, *130*, 836-838. (c) Tsuda, A.; Nakamura, T.; Sakamoto, S.; Yamaguchi, K.; Osuka, A. *Angew. Chem. Int. Ed.* **2002**, *41*,

2817-2821. (d) Gao, Y; Zhang, X.; Ma, C.; Li, X.; Jiang, J. *J. Am. Chem. Soc.* **2008**, *130*, 17044-17052. (e) Hajjaj, F.; Yoon, Z. S.; Yoon, M.-C.; Park, J.; Satake, A.; Kim, D.; Kobuke, Y. *J. Am. Chem. Soc.* **2006**, *128*, 4612-4623. (f) Fujisawa, K.; Satake, A.; Hirota, S.; Kobuke, Y. *Chem. Eur. J.* **2008**, *14*, 10735-10744.

6. (a) Kishida, T.; Fujita, N.; Sada, K.; Shinkai, S. *J. Am. Chem. Soc.* **2005**, *127*, 7298-7299. (b) Shirakawa, M.; Kawano, S.; Fujita, N.; Sada, K.; Shinkai, S. *J. Org. Chem.* **2003**, *68*, 5037-5044. (c) Kawano, S.; Tamaru, S.; Fujita, N.; Shinkai, S. *Chem. Eur. J.* **2004**, *10*, 343-351.

7. (a) Escudero, C.; Crusats, J.; Díez-Pérez, I.; El-Hachemi, Z.; Ribó, J. M. *Angew. Chem. Int. Ed.* **2006**, *45*, 8032-8035. (b) Lee, S. J.; Malliakas, C. D.; Kanatzidis, M. G.; Hupp, J. T.; Nguyen, S. T. *Adv. Mater.* **2008**, *20*, 3543-3549. (c) Kano, K.; Fukuda, K.; Wakami, H.; Nishiyabu, R.; Pasternack, R. F. *J. Am. Chem. Soc.* **2000**, *122*, 7494-7502. (d) van Hameren, R.; Schön, P.; van Buul, A. M.; Hoogboom, J.; Lazarenko, S. V.; Gerritsen, J. W.; Engelkamp, H.; Christianen, P. C. M.; Heus, H. A.; Maan, J. C.; Rasing, T.; Speller, S.; Rowan, A. E.; Elemans, J. A. A. W.; Nolte, R. J. M. *Science*, **2006**, *314*, 1433-1436.

8. *The Porphyrin Handbook*, Vol. 6, Kadish, K. M.; Smith, K. M.; Guilard, R. Eds.; Academic Press; Sandiego, 2000.

9. (a) Shimizu, T.; Masuda, M.; Minamikawa, H. *Chem. Rev.* **2005**, *105*, 1401-1443. (b) Hill, J. P.; Jin, W.; Kosaka, A.; Fukushima, T.; Ichihara, H.; Shimomura, T.; Ito, K.; Hashizume, T.; Ishii, N.; Aida, T. *Science*, **2004**, *304*, 1481-1483. (c) Yamamoto, Y.; Fukushima, T.; Suna, Y.; Ishii, N.; Saeki, A.; Seki, S.; Tagawa, S.; Taniguchi, M.; Kawai, T.; Aida, T. *Science*, **2006**, *314*, 1761-1764. (d) El

Hamaoui, B.; Zhi, L.; Pisula, W.; Kolb, U.; Wu, J.; Müllen, K. *Chem. Commun.* **2007**, 2384-2386. (e) Zhang, X.; Chen, Z.; Würthner, F. *J. Am. Chem. Soc.* **2007**, *129*, 4886-4887. (f) Che, Y.; Datar, A.; Balakrishnan, K.; Zang, L. *J. Am. Chem. Soc.* **2007**, *129*, 7234-7235. (g) Kim, J.-K.; Lee, E.; Lee, M. *Angew. Chem. Int. Ed.* **2006**, *45*, 7195-7198. (h) Sakurai, T.; Shi, K.; Sato, H.; Tashiro, K.; Osuka, A.; Saeki, A.; Seki, S.; Tagawa, S.; Sasaki, S.; Masunaga, H.; Osaka, K.; Takata, M.; Aida, T. *J. Am. Chem. Soc.* **2008**, *130*, 13812-13813. (i) Ishizuka, T.; Isono, Y.; Jiang, D.-L.; Tanaka, H. *submitted*.

10. (a) Israelachvili, J. *Intermolecular and Surface Forces*, 2nd ed.; Academic Press: San Diego, CA, 1991. (b) $P_c = v/al$, where v is the effective molecular volume, a is the occupied area by hydrophilic chains, and l is optimal molecular length.

11. (a) Osuka, A.; Shimidzu, H. *Angew. Chem. Int. Ed. Engl.* **1997**, *36*, 135-137. (b) Aratani, N.; Takagi, A.; Yanagawa, Y.; Matsumoto, T.; Kawai, T.; Yoon, Z.S.; Kim, D.; Osuka, A. *Chem. Eur. J.* **2005**, *11*, 3389-3404.

Chapter 2.

Syntheses of Triethyleneglycol(TEG)-Tethered and Alkyl-Tethered Dipyrromethanes

Published in *Tetrahedron Lett*. **2009**, *50*, 7137–7140.

Masafumi Oda, Tomoya Ishizuka, Shigeo Arai, Atsushi Takano, and Donglin Jiang

2-1 Synthesis of a Triethyleneglycol(TEG)-Tethered Dipyrromethane

The synthesis of 3,7-bis(TEGO)dipyrromethane **6** has been accomplished from N-tosylglycine as the starting material (Scheme 2-1). As shown in Scheme 1-1, the most critical step of this procedure is the pyrrole cyclization reaction but the synthesis of ethyl 4-alkoxy-pyrrole-2(and 3)-carboxylate has been rarely investigated. Recently, Vyas *et al*. have reported a newly-developed one-pot synthesis of 4-alkoxypyrrole with intramolecular Wittig reaction from a corresponding N-tosyl derivative of an α-amino acid ester,[1] and this method is employed for the synthesis of a key intermediate, diethyl 4-(TEGO)-pyrrole-2,3-dicarboxylate **4**. The reaction yield of the synthesis of **4** was quite good (83%) and only 2 steps are required for obtaining the TEG-tethered pyrrole. 1,2,8,9-tetrakis(ethoxycarbonyl)-3,7-bis(TEGO)dipyrromethane **5** was obtained by the condensation reaction of pyrrole **4**,[2] and the synthesis of the target TEG tethered-dipyrromethane **6** was accomplished by two-step decarboxylation, hydrolysis under basic condition and subsequent heating.[3] Noteworthy, the decarboxylated dipyrromethane **6** was not so unstable even in air and can be kept during several months in refrigerator at -40 ºC. Vilsmeier formylation of **6** did not give 1,9-formyl-3,7-bis(TEGO)dipyrromethane to be a reaction intermediate for synthesis of asymmetrical porphyrins, and consequently functionalization of alkyl-tethered dipyrromethane was necessary (Chapter 2-2).

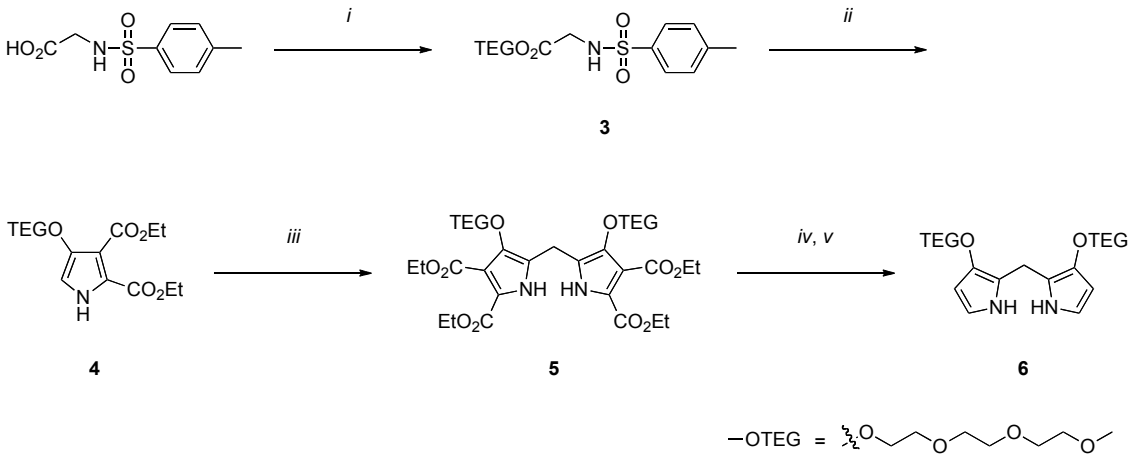

Scheme 2-1. Synthesis of TEG-tethered dipyrromethane **6**. (*i*) $CH_3(OCH_2CH_2)_3OH$, *p*-TsOH, xylene, reflux, 7 h, 89%.; (*ii*) 1) PPh_3, diethyl acetylenedicarboxylate, dioxane, r. t., 1 h then reflux, 12 h.; 2) DBU, 90 ºC, 2 h, 83%.; (*iii*) BF_3OEt_2, $CH_2(OMe)_2$, CH_2Cl_2, r. t., 16 h, 94%.; (*iv*) NaOH (aq), EtOH, reflux, 5 h.; (*v*) $H_2N(CH_2)_2OH$, 120 ºC, 2 h, 2 steps: 49%.

2-2 Synthesis of an Alkyl-Tethered Dipyrromethane

The synthesis of the key intermediate of ethyl 4-dodecyl-pyrrole-2-carboxylate **10** for the synthesis of 3,7-bis(dodecyl)dipyrromethane **12** has been carried out by two different routes; one is traditional Barton–Zard reaction (Route 1) and the other is based on Friedel–Crafts reaction (Route 2; Scheme 2-2). In this time, because Route 2 could not be employed for target porphyrin synthesis due to the technical problem occurred in the following reaction, the porphyrin was synthesized by a tough procedure of Route 1.

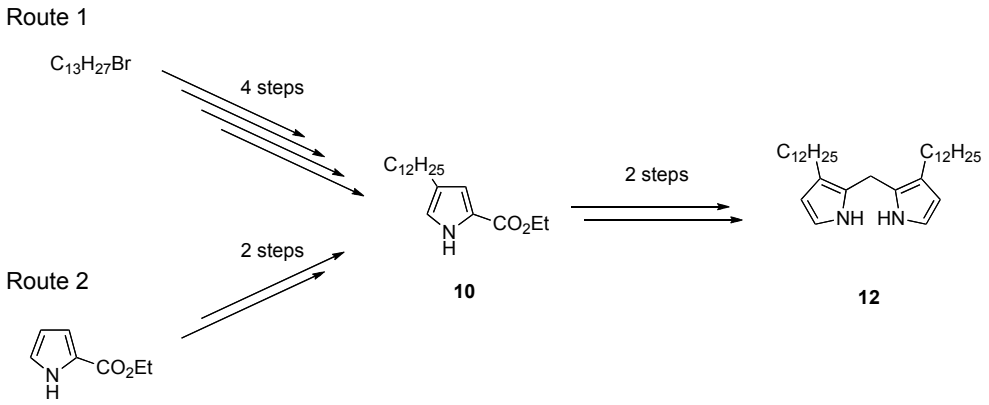

Scheme 2-2. Two different synthetic routes for compound **10** and **12**.

2-2-1 Route 1: From Barton–Zard Pyrrole Synthesis

I employed the reported procedure of 1-nitrotridecane **7** from 1-bromotridecane,[4] and Henry reaction and following acetylation afforded 2-nitrotetradecan-1-ol **8** and 2-nitrotetradecyl acetate **9**, respectively.[5] Unfortunately, ethyl 4-dodecyl-pyrrole-2-carboxylate **10** was obtained in only 26% yield despite of various efforts, although the Barton–Zard synthesis usually give a target pyrrole in more than 60% yield.[5, 6] 3,7-Bis(dodecyl)dipyrromethane **12** was synthesized by acid catalyzed condensation of alkyl-tethered pyrrole **10** with dimethoxymethane[2] and subsequent decarboxylation[7] but this alkyl-tethered dipyrromethane **12** was a little unstable in air and thus it had to be used immediately after synthesis for next step. Dipyrromethane **12** was functionalized at the α-positions for the synthesis of the target asymmetric porphyrin and the functionalization started from formylation reaction.[8] In this case, Vilsmeier reaction gave 3,7-didodecyl-1,9-diformyldipyrromethane **13** in 83% yield and then formyl groups were transformed into hydroxymethyl (Chapter 3-5) or imino groups (**15**).[9]

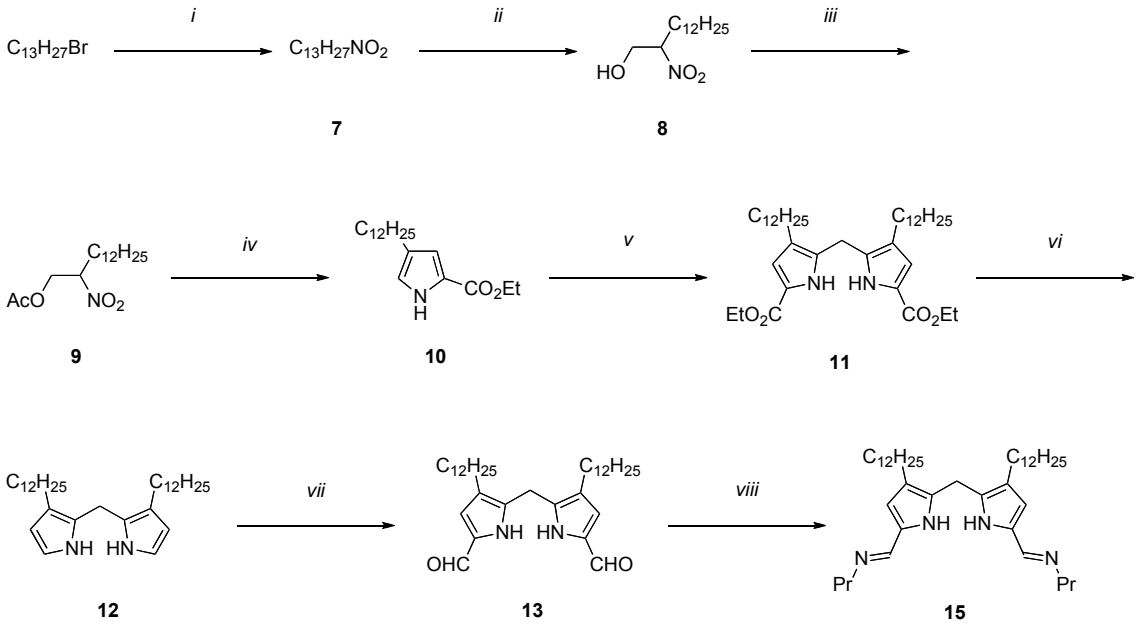

Scheme 2-3. Synthesis of alkyl-tethered dipyrromethane **15** (Roure 1). (*i*) $AgNO_2$, Et_2O, r. t., 4 days, 76%.; (*ii*) Et_3N, HCHO (aq), CH_3CN, 0 ºC, 30 min then r. t., 15 h, 62%.; (*iii*) pyridine, Ac_2O, 1 h, 99%.; (*iv*) EtO_2CCH_2NC, K_2CO_3, THF, EtOH, 60 ºC, 65 h, 26%.; (*v*) $BF_3{\cdot}OEt_2$, $CH_2(OMe)_2$, CH_2Cl_2, 0 ºC, 36 h, 55%.; (*vi*) NaOH (aq), $(CH_2OH)_2$, 180 ºC, 1 h, 83%.; (*vii*) 1) $POCl_3$, DMF, CH_2Cl_2, 0 ºC, 3 h.; 2) Na_2CO_3 (aq), r. t., 15.5 h, 83%.; (*viii*) *n*-$PrNH_2$, THF, r. t., 1 h, 99%.

2-2-2 Route 2: From Friedel–Crafts Reaction

Murakami *et al*. have reported *β*-acylation of ethyl pyrrole-2-carboxylate by Friedel–Crafts acylation and reduction of acylpyrrole with triethylsilane in trifluoroacetic acid.[10] Ethyl 4-dodecyl-pyrrole-2-carboxylate **10** was also obtained from this synthetic methodology in very good yield (total 98% in 2 steps, Scheme 2-4). However, 3,7-Bis(dodecyl)dipyrromethane **12** obtained from this procedure could not be fomylated with same procedure as Route 1. This problem is probably just technical matter and Route 2 must be utilized for porphyrin synthesis if this is cleared.*

* The elemental analysis data for dipyrromethane **11** obtained from this route matches to the theoretical value (*vide infra*), which indicates the high purity of the dipyrro-methane.

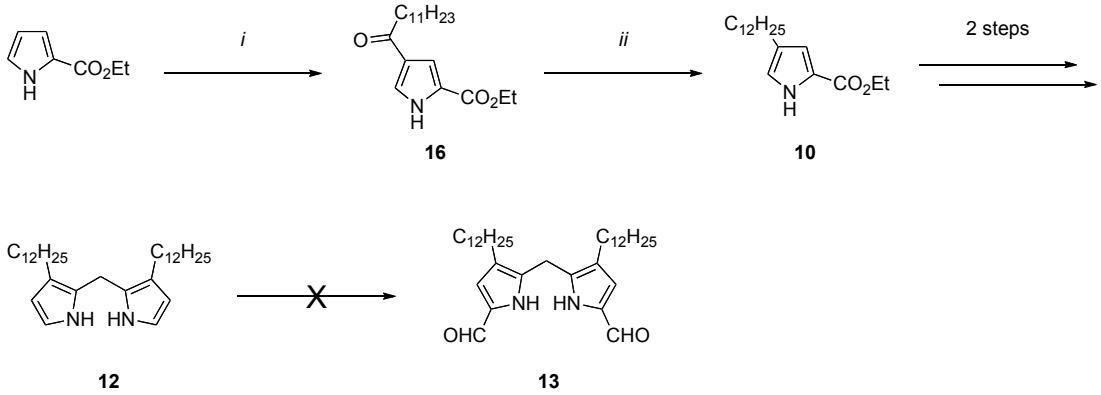

Scheme 2-4. Synthesis of alkyl-tethered dipyrromethane **12** (Route 2). (*i*) $C_{11}H_{23}COCl$, $AlCl_3$, 1,2-dichloroethane, reflux, 1 h, quant.; (*ii*) Et_3SiH, TFA, r. t., 4 h, 98%.

2-3 Conclusion

The syntheses of TEG-tethered and alkyl-tethered dipyrromethanes was successfully accomplished but the synthetic route of alkyl-tethered one needs further improvement on the total reaction yield and the number of steps. The present methodology should be valuable for preparing various molecular designs for *β*-substituted porphyrin complexes.

2-4 Experimental Section

General. THF was freshly distilled over benzophenone ketyl under Ar before use. Diethyl ether, dioxane, 1,2-dichloroethane, dichloromethane and ethanol were distilled over calcium hydride under Ar. DMF was distilled over anhydrous magnesium sulfate *in vacuo* and methanol was distilled under Ar before use. Potassium carbonate was grinded and dried at 120 ℃ for 3 days. Triphenylphosphine, triethyl silane, 1-bromotridecane, triethyleneglycol monomethylether and boron trifluoride diethyletherate were obtained from Tokyo Kasei Co. (TCI). Potassium carbonate, sodium carbonate, triethylamine, pyridine and ethylene glycol were purchased from Kanto Chemicals. N-tosylglycine, lauroyl chloride, ethyl pyrrole-2-carboxylate, 2-aminoethanol, dimethoxymethane, phosphoryl chloride, diethyl acetylenedicarboxylate, *p*-toluenesulfonic acid monohydrate, hydrochloric acid and

sodium hydroxide were obtained from Wako Pure Chemical Industries. Silver nitrite, aluminum chloride, ethyl isocyanoacetate, 37% formaldehyde (aq), 1,8-diazabicyclo[5.4.0]undec-7-ene (DBU), trifluoroacetic acid and glacial acetic acid were purchased from Aldrich. *n*-Propylamine, acetic anhydride, sodium sulfate, sodium bicarbonate and ammonium chloride were obtained from Nacalai Tesque. Column chromatography was performed on the bench top, using silica gel (Wakogel C–300HG) or aluminum oxide (Gamma alumina KCG-1525W). All deuterated solvents for NMR measurement were used as received from Cambridge Isotope Laboratories, Inc. 1-Nitrotridecane **7** were prepared according to a reported procedure.[4]

^{1}H NMR spectrum were recorded on a JEOL model JNM–LA400 or JNM-LA500 NMR spectrometer, where chemical shifts (δ in ppm) were determined with residual proton signals of the solvent as standard. All *J* values are reported in Hertz. Matrix–assisted laser desorption ionization time–of–flight mass (MALDI–TOF MS) spectroscopic data were obtained with an Applied Biosystems BioSpectrometry model Voyager–DE–STR spectrometer in reflector or linear mode. Samples were prepared as micromolar solutions in dichloromethane or THF, and dithranol (Aldrich) was utilized as the matrix. Fast atom bombardment mass spectra (FAB-MS) and high-resolution mass spectra were recorded on a JEOL model JMS-700 spectrometer in the positive ion mode with a xenon primary atom beam with 3-nitrobenzylalcohol matrix. Infrared (IR) spectra were recorded on a JASCO model FT IR–6100 Fourier transform infrared spectrometer.

2-(2-(2-Methoxyethoxy)ethoxy)ethyl 2-(4-methylphenylsulfonamido)acetate (3). A mixture of N-tosylglycine (3.90 g, 17.0 mmol), triethyleneglycol monomethyl

ether (16.0 mL, 102 mmol), and *p*-toluenesulfonic acid monohydrate (0.1619 g, 0.8511 mmol) in xylene (39 mL) was refluxed for 7 h under Ar. After cooling to room temperature, the reaction mixture was washed with sat. sodium bicarbonate (aq), and the aqueous phase was extracted with toluene. The combined organic phase was dried over sodium sulfate, filtered, and evaporated *in vacuo*. The residue was purified by column chromatography on silica gel eluted with ethyl acetate, the first fraction was collected, and the solvent was evaporated under vacuum to afford the product **3** (5.6764 g, 15.119 mmol) as a pale yellow liquid in 89% yield. ^{1}H NMR ($CDCl_3$): δ 7.75 (d, 2H, J = 8.3 Hz), 7.31 (d, 2H, J = 8.5 Hz), 5.21 (t, 1H, J = 5.4 Hz), 4.18 (t, 2H, J = 4.8 Hz), 3.81 (d, 2H, J = 5.6 Hz), 3.64-3.61 (m, 8H), 3.55-3.53 (m, 2H), 3.37 (s, 3H), 2.42 (s, 3H). HRMS: m/z = 376.1437 (calcd. for $C_{16}H_{26}NO_7S$ $[M+H]^+$ = 376.1430).

Diethyl 4-(2-(2-(2-methoxyethoxy)ethoxy)ethoxy)-1*H*-pyrrole-2,3-dicarboxylate (4). To a predried mixture of **3** (0.8128 g, 2.165 mmol) and triphenylphosphine (0.7101 g, 2.707 mmol) in a 50 mL round bottom flask was injected dry dioxane (4.33 mL) under Ar. Diethyl acetylenedicarboxylate (0.42 mL, 2.6 mmol) was added dropwise to the reaction mixture at 0 ºC and then the ice bath was removed to allow the mixture to warm up to room temperature. After stirring for 1 h, the mixture was brought to reflux and kept at the temperature for 12 h. The temperature was lowered to 90 ºC and DBU (0.65 mL, 4.3 mmol) was added. Two hour later, the mixture was allowed to cool to room temperature and the solvent was removed under vacuum. The residue was purified by column chromatography on silica gel eluted first with chloroform-acetone (5:1) and then with chloroform-methanol (10:1). The fourth fraction was collected and the solvent was evaporated to afford the product **4** (0.6670 g, 1.786 mmol) as a pale yellow liquid in 83% yield. ^{1}H NMR ($CDCl_3$): δ 8.90 (bs, 1H),

6.61 (d, 1H, J = 3.2 Hz), 4.35-4.31 (m, 4H), 4.07 (t, 2H, J = 4.9 Hz), 3.80 (t, 2H, J = 4.9 Hz), 3.71-3.70 (m, 2H), 3.66-3.64 (m, 4H), 3.57-3.55 (m, 2H), 3.39 (s, 3H), 1.36-1.33 (m, 6H). HRMS: m/z = 373.1744 (calcd. for $C_{17}H_{27}NO_8$ $[M]^+$ = 373.1737).

1,2,8,9-Tetrakis(ethoxycarbonyl)-3,7-bis(2-(2-(2-methoxyethoxy)ethoxy) ethoxy)dipyrromethane (5). To the predried **4** (0.25 g, 0.67 mmol) in a 50 mL round bottom flask were injected dry dichloromethane (6.1 mL) and dimethoxymethane (0.29 mL, 3.3 mmol) under Ar. Boron trifluoride diethyletherate (0.05 mL, 0.4 mmol) was added and the reaction mixture was stirred at room temperature for 16 h. The solvent was removed under vacuum, and the residue was added to sat. sodium bicarbonate (aq) (20 mL) and extracted with dichloromethane (20 mL, 3 times). The combined organic phase was dried over anhydrous sodium sulfate, filtered, and the solvent was evaporated *in vacuo* to afford the product **5** (0.2394 g, 0.3155 mmol) as a yellow liquid in 94% yield. ^{1}H NMR ($CDCl_3$): δ 10.67 (bs, 2H), 4.31-4.26 (m, 8H), 4.15-4.13 (m, 4H), 3.98 (s, 2H), 3.84-3.82 (m, 8H), 3.75-3.73 (m, 4H), 3.55-3.54 (m, 4H), 3.40-3.39 (m, 4H), 3.29 (s, 6H), 1.34-1.30 (m, 12H). HRMS: m/z = 758.3483 (calcd. for $C_{35}H_{54}N_2O_{16}$ $[M]^+$ = 758.3473).

3,7-Bis(2-(2-(2-methoxyethoxy)ethoxy)ethoxy)dipyrromethane (6). To the predried **5** (0.4296 g, 0.5661 mmol) in a 50 mL round bottom flask were injected ethanol (6.58 mL) and 7.5 M sodium hydroxide (aq) (0.66 mL, 4.9 mmol) under Ar. The reaction mixture was refluxed for 5 h and then allowed to cool to room temperature, and glacial acetic acid (0.34 mL, 5.9 mmol) was added to the mixture at 0 ºC. The solvent was removed under vacuum overnight, and 2-aminoethanol (2.0 mL) was added to the residual solid. The suspension was heated to 120 ºC for 2 h and the solvent was removed at 50 ºC under vacuum. Brine (25 mL) was added to the residue, and the

mixture was extracted with ethyl acetate (25 mL, 3 times). The combined organic phase was dried over anhydrous sodium sulfate, filtered, and the volatiles were evaporated *in vacuo*. The crude material was purified by column chromatography on aluminum oxide (activity III) eluted with ethyl acetate, and the first fraction was collected and the solvent was removed under vacuum to afford the product **6** (0.1292 g, 0.2746 mmol) as a brown liquid in 49% yield. ^{1}H NMR ($CDCl_3$): δ 9.03 (bs, 2H), 6.38 (t, 2H, J = 3.1 Hz), 5.83 (t, 2H, J = 2.9 Hz), 4.08-4.06 (m, 4H), 3.84 (s, 2H), 3.77-3.73 (m, 12H), 3.65-3.64 (m, 4H), 3.53-3.51 (m, 4H), 3.34 (s, 6H). HRMS: m/z = 470.2627 (calcd. for $C_{23}H_{38}N_2O_8$ $[M]^+$ = 470.2628).

2-Nitrotetradecan-1-ol (8). 1-Nitrotridecane **7** was prepared from 1-bromotridecane with silver(I) nitrite in dry diethyl ether according to the literature procedure.[1,2] To a stirred solution of **7** (34.15 g, 148.9 mmol) in acetonitrile (60.7 mL) were added dropwise the acetonitrile solution (86.4 mL) of triethylamine (2.1 mL, 15 mmol) and 37% formaldehyde (aq) (11.1 mL, 149 mmol) at 0 ºC under Ar. Thirty min later, ice bath was removed to allow the mixture to warm up to room temperature and the reaction mixture was stirred for further 15 h. The mixture was poured into sat. ammonium chloride (aq) (400 mL) and extracted with hexane (600 mL, 3 times). The combined organic phase was washed with brine, dried over anhydrous sodium sulfate, filtered, and the solvent was evaporated *in vacuo*. The residue was purified by column chromatography on silica gel eluted with hexane-ethyl acetate (6:1), and the second fraction was collected and the solvent was evaporated under vacuum to afford the product **8** (23.88 g, 92.07 mmol) as a pale yellow liquid in 62% yield, accompanied with the recovered starting material **7** (6.61 g, 19%). ^{1}H NMR ($CDCl_3$): δ 4.63-4.57 (m, 1H), 4.07-4.01 (m, 1H), 3.91 (d, 1H, J = 12.9 Hz), 1.99-1.94 (m, 2H), 1.81-1.72 (m,

1H), 1.25 (bs, 20H), 0.88 (t, 3H, J = 6.7 Hz). HRMS: m/z = 260.2218 (calcd. for $C_{14}H_{30}NO_3$ $[M+H]^+$ = 260.2226). FTIR (KBr): ν [cm^{-1}] 3386, 2925, 2854, 1555, 1467, 1363, 1332, 1061, 862, 721.

2-Nitrotetradecyl acetate (9). To a stirred solution of **8** (23.88 g, 92.06 mmol) in acetic anhydride (94.5 mL) were added dropwise pyridine (7.3 mL, 92 mmol) at 0 ºC under Ar. One hour later, the reaction mixture was poured into sat. sodium bicarbonate (aq) (500 mL) at 0 ºC and extracted with hexane (500 mL, 3 times). The combined organic phase was washed with sat. sodium bicarbonate (aq) and brine, dried over anhydrous sodium sulfate, filtered, and evaporated *in vacuo* to give the product **9** (27.54 g, 91.37 mmol) as a colorless liquid in 99% yield. ^{1}H NMR ($CDCl_3$): δ 4.74-4.68 (m, 1H), 4.41-4.37(m, 2H), 2.06 (s, 3H), 2.00-1.90 (m, 1H), 1.75-1.72 (m, 1H), 1.25 (bs, 20H), 0.88 (t, 3H, J = 6.8 Hz). HRMS: m/z = 302.2328 (calcd. for $C_{16}H_{32}NO_4$ $[M+H]^+$ = 302.2331). FTIR (KBr): ν [cm^{-1}] 2925, 2855, 1751, 1558, 1456, 1368, 1226, 1048.

Ethyl 4-dodecyl-1*H*-pyrrole-2-carboxylate (10).

<Route 1> To a predried **9** (6.22 g, 20.6 mmol) in a 100 mL round bottom flask were injected dry THF (25 mL) and dry ethanol (25 mL) under Ar. Ethyl isocyanoacetate (2.3 mL, 21 mmol) and grinded potassium carbonate (5.69 g, 41.2 mmol) were added and then the reaction mixture was stirred at 60 ºC for 78 h. After cooling to room temperature, the mixture was poured into water (160 mL), neutralized by addition of 1 M hydrochloric acid at 0 ºC, and extracted with diethyl ether (200 mL, 3 times). The combined organic phase was dried over anhydrous sodium sulfate, filtered, and the solvent was evaporated *in vacuo*. The residue was purified by column chromatography on silica gel eluted with hexane-ethyl acetate (10:1), and the fourth fraction was collected and the solvent was evaporated under vacuum to afford the

product **10** (1.67 g, 5.43 mmol) as a pale yellow solid in 26% yield.

<Route 2> To a stirred solution of **16** (4.50 g, 14.0 mmol) in trifluoroacetic acid (56.4 mL) were added dropwise triethyl silane (8.72 mL, 54.6 mmol) at room temperature under Ar. Four hours later, half amount of the solvent was evaporated and the mixture was poured into sat. sodium bicarbonate (aq) (650 mL). The mixture was extracted with ethyl acetate (150 mL, 3 times) and the combined organic phase was washed with brine, dried over anhydrous sodium sulfate, filtered, and evaporated *in vacuo*. The residue was purified by column chromatography on silica gel eluted with hexane-ethyl acetate whose ratio was gradually changed from 15:0 to 15:1. The second fraction was collected and the solvent was evaporated under vacuum to afford the product **10** (4.23 g, 13.8 mmol) as a pale orange solid in 98% yield.

^{1}H NMR ($CDCl_3$): δ 8.86 (bs, 1H), 6.76 (s, 1H), 6.72 (s, 1H), 4.30 (q, 2H, J = 7.2 Hz), 2.44 (t, 2H, J = 7.7 Hz), 1.57-1.54 (m, 2H), 1.36-1.25 (m, 21H), 0.88 (t, 3H, J = 6.8 Hz). HRMS: m/z = 307.2517 (calcd. for $C_{19}H_{33}NO_2$ $[M]^+$ = 307.2511).

3,7-Didodecyl-1,9-bis(ethoxycarbonyl)dipyrromethane (11). To a predried **10** obtained from Route 1 (2.11 g, 6.86 mmol) in a 200 mL round bottom flask were injected dry dichloromethane (62 mL) and dimethoxymethane (3.0 mL, 34 mmol) under Ar. Boron trifluoride diethyletherate (0.53 mL, 4.2 mmol) was added at 0 °C and the reaction mixture was stirred at 0 ºC for 36 h. The mixture was poured into sat. sodium bicarbonate (aq) (200 mL) and extracted with chloroform (500 mL, 3 times). The combined organic phase was washed with brine, dried over anhydrous sodium sulfate, filtered, and evaporated *in vacuo*. The residual solid was washed with hexane and the precipitate was collected by centrifugation to give the product **11** (1.18 g, 1.88 mmol) as a colorless solid in 55% yield. ^{1}H NMR ($CDCl_3$): δ 9.09 (bs, 2H), 6.74 (d, 2H, J = 2.4

Hz), 4.26 (q, 4H, *J* = 7.1 Hz), 3.89 (s, 2H), 2.38 (t, 4H, *J* = 7.7 Hz), 1.52-1.50 (m, 4H), 1.30-1.28 (m, 42H), 0.88 (t, 6H, *J* = 6.8 Hz). HRMS: *m/z* = 626.5011 (calcd. for $C_{39}H_{66}N_2O_4$ $[M]^+$ = 626.5023). Pyrrole **10** obtained from Route 2 was also condensed with dimethoxymethane to afford same product **11**. Elemental analysis of this product was examined. Anal.: calcd. for $C_{39}H_{66}N_2O_4$; C, 74.71. H, 10.61. N, 4.47. found; C, 74.65. H, 10.71. N, 4.46.

3,7-Bis(dodecyl)dipyrromethane (12). To the solution of **11** obtained from Route 1 (0.4034 g, 0.6434 mmol) in ethylene glycol (3.2 mL) in a 50 mL round bottom flask was added 20 M sodium hydroxide (aq) (0.4 mL), and the mixture was degassed by repeated freeze-pump-thaw cycles, and stirred at 180 ºC for 1 h under Ar. Water (30 mL) was added to quench the reaction, and the reaction mixture was neutralized into pH 7 by addition of 1 M hydrochloric acid (aq) at 0 ºC and extracted with chloroform (60 mL, 3 times). The combined organic phase was washed with brine, dried over anhydrous sodium sulfate, filtered, and evaporated *in vacuo* to give a brown solid of **12** (0.2584 g, 0.5352 mmol) in 83% yield. Dipyrromethane **11** obtained from Route 2 was also decarboxylated with the same procedure and the result of this synthesis was almost identical. The obtained **12** was used without further purification. ^{1}H NMR ($CDCl_3$): δ 7.61 (bs, 2H), 6.58 (t, 2H, *J* = 2.7 Hz), 6.05 (t, 2H, *J* = 2.7 Hz), 3.85 (s, 2H), 2.43 (t, 4H, *J* = 7.7 Hz), 1.57-1.53 (m, 4H), 1.26 (bs, 36H), 0.88 (t, 6H, *J* = 6.8 Hz). HRMS: *m/z* = 481.4535 (calcd. for $C_{33}H_{57}N_2$ $[M-H]^+$ = 481.4522).

3,7-Didodecyl-1,9-diformyldipyrromethane (13). A Vilsmeier reagent was prepared by adding phosphoryl chloride (0.02 mL, 0.2 mmol) dropwise to dry DMF (0.13 mL) at 0 ºC under Ar and stirring for 30 min at the temperature. To a predried **12** obtained from Route 1 (43.0 mg, 0.0891 mmol) in the 50 mL round bottom flask was

injected dry dichloromethane (1.0 mL) under Ar, subsequently cooled to 0 °C, and then to the solution was added dropwise the Vilsmeier reagent. The reaction mixture was stirred at 0 ºC for 3 h and sat. sodium carbonate (aq) (3.3 mL) was added and the ice bath was removed to allow the mixture to warm up to room temperature. After stirring for 4.5 h, sodium carbonate (0.3570 g) was added and the mixture was stirred for further 11 h. The suspension was extracted with dichloromethane (10 mL, 3 times) and the organic phase was washed with water, dried over anhydrous sodium sulfate, and filtered. The solvent was evaporated *in vacuo* to afford the product **13** (40.0 mg, 74.2 μmol) as a brown solid in 83% yield. Dipyrromethane **12** obtained from Route 2 could not be transformed into **13** from the same procedure and the reaction just resulted in the decomposition of the starting material. ^{1}H NMR ($CDCl_3$): δ 10.67 (bs, 2H), 9.37 (s, 2H), 6.80 (s, 2H), 3.98 (s, 2H), 2.45 (t, 4H, J = 7.8 Hz), 1.55 (t, 4H, J = 7.0 Hz), 1.26 (bs, 36H), 0.88 (t, 6H, J = 6.8 Hz). HRMS: m/z = 538.4484 (calcd. for $C_{35}H_{58}N_2O_2$ $[M]^+$ = 538.4498).

3,7-Didodecyl-1,9-bis[(propylimino)methyl]dipyrromethane (15). A solution of **13** (20.0 mg, 37.1 μmol) and *n*-propylamine (7.6 μL, 92 μmol) in dry THF (0.19 mL) was stirred at room temperature for 1.5 h under nitrogen. Removal of the solvent and excess *n*-propylamine *in vacuo* gave the product **15** (22.8 mg, 36.7 μmol) as a brown solid in 99% yield, which was stored under Ar and used without further purification. ^{1}H NMR ($CDCl_3$): δ 7.86 (s, 2H), 6.25 (s, 2H), 3.84 (s, 2H), 3.40 (t, 4H, J = 7.0 Hz), 2.37 (t, 4H, J = 7.6 Hz), 1.63-1.59 (m, 4H), 1.51-1.49 (m, 4H), 1.26 (bs, 36H), 0.90-0.87 (m, 12H). HRMS: m/z = 621.5822 (calcd. for $C_{41}H_{73}N_4$ $[M+H]^+$ = 621.5835).

Ethyl 4-(1-oxododecyl)-1*H*-pyrrole-2-carboxylate (16). To a stirred solution of

aluminum chloride (14.13 g, 106 mmol) and lauroyl chloride (24.5 mL, 106 mmol) in dry 1,2-dichloroethane (70.6 mL) were added dropwise the dry 1,2-dichloroethane solution (70.6 mL) of ethyl pyrrole-2-carboxylate (3.69 g, 26.5 mmol) at 0 ºC under Ar and the mixture was refluxed for 1 h. The mixture was poured into sat. sodium bicarbonate (aq) (700 mL) and the colorless solid was removed by vacuum filtration. The filtrate was extracted with ethyl acetate (400 mL, 4 times) and the combined organic phase was washed with sat. sodium bicarbonate (aq), water and brine. The mixture was dried over anhydrous sodium sulfate, filtered and evaporated *in vacuo*, and the residual solid was purified by column chromatography on silica gel eluted with dichloromethane-methanol whose ratio was gradually changed from 50:0 to 50:1. The second fraction was collected and the solvent was evaporated under vacuum to afford the product **16** (9.21 g, 28.7 mmol) as a pale yellow solid in quantitative yield. ^{1}H NMR ($CDCl_3$): δ 9.53 (bs, 1H), 7.53 (dd, 1H, J = 3.2, 1.7 Hz), 7.29 (dd, 1H, J = 2.4, 1.7 Hz), 4.35 (q, 2H, J = 7.2 Hz), 2.75 (t, 2H, J = 7.5 Hz), 1.70-1.64 (m, 2H), 1.34-1.30 (m, 19H), 0.87 (t, 3H, J = 6.8 Hz). HRMS: m/z = 322.2385 (calcd. for $C_{19}H_{32}NO_3$ $[M+H]^+$ = 322.2382).

2-5 References

1. Mastalerz, H.; Gavai, A. V.; Fink, B.; Struzynski, C.; Tarrant, J.; Vite, G. D.; Wong, T. W.; Zhang, G.; Vyas, D. M. *Can. J. Chem.* **2006**, *84*, 528-533.

2. Tang, J.; Verkade, J. G. *J. Org. Chem.* **1994**, *59*, 7793-7802.

3. Abdalmuhdi, I.; Chang, C. K. *J. Org. Chem.* **1985**, *50*, 411-413.

4. (a) Woodcock, S. R.; Marwitz, A. J. V.; Bruno, P.; Branchaud, B. P. *Org. Lett.* **2006**, *8*, 3931-3934. (b) White, A. D.; Purchase, C. F. II; Picard, J. A.; Anderson, M. K.; Mueller, S. B.; Bocan, T. M. A.; Bousley, R. F.; Hamelehle, K. L.; Krause, B. R.; Lee, P.; Stanfield, R. L.; Reindel, J. F. *J. Med. Chem.* **1996**, *39*, 3908-3919.

5. Fumoto, Y.; Eguchi, T.; Uno, H.; Ono, N. *J. Org. Chem.* **1999,** *64,* 6518-6521.

6. Roth, S. D.; Shkindel, T.; Lightner, D. A. *Tetrahedron* **2007**, *63*, 11030-11039.

7. Chang, C. J.; Deng, Y.; Peng, S.-M.; Lee, G.-H.; Yeh, C.-Y.; Nocera, D. G. *Inorg. Chem.* **2002**, *41*, 3008-3016.

8. Wickramasinghe, A.; Jaquinod, L.; Nurco, D. J.; Smith, K. M. *Tetrahedron* **2001**, *57*, 4261-4269.

9. Taniguchi, M.; Balakumar, A.; Fan, D.; McDowell, B. E.; Lindsey, J. S. *J. Porphyrins Phthalocyanines* **2005**, *9*, 554-574.

10. (a) Tani, M.; Ariyasu, T.; Nishiyama, C.; Hagiwara, H.; Watanabe, T.; Yokoyama, Y.; Murakami, Y. *Chem. Pharm. Bull.* **1996**, *44*, 48-54. (b) Tani, M.; Ariyasu, T.; Ohtsuka, M.; Koga, T.; Ogawa, Y.; Yokoyama, Y.; Murakami, Y. *Chem. Pharm. Bull.* **1996**, *44*, 55-61.

Chapter 3.

Syntheses of Amphiphilic β-Alkylporphyrin Complexes

Published in *Tetrahedron Lett*. **2009**, *50*, 7137–7140.

Masafumi Oda, Tomoya Ishizuka, Shigeo Arai, Atsushi Takano, and Donglin Jiang

3-1 Possible Synthetic Routes of Target Porphyrin

In contrast to the synthesis of *meso*-aryl-type porphyrin, that of asymmetrically substituted *β*-alkyl-type porphyrin has not been well explored.[1] Herein, several conditions were examined for the condensation reaction of two different dipyrromethanes, so called MacDonald-type 2 + 2 condensation (Scheme 3-1).

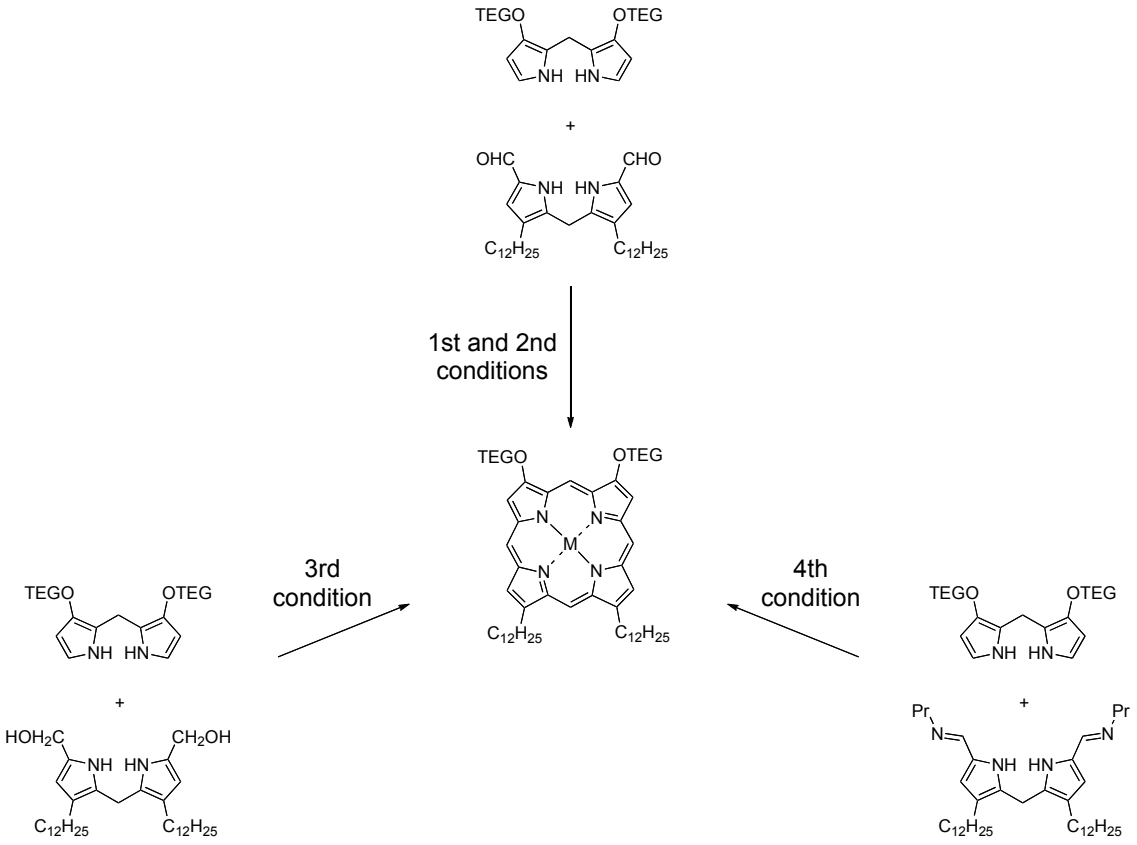

Scheme 3-1. Possible synthetic routes of target asymmetric porphyrin **1**-M from MacDonald-type 2 + 2 condensation.

3-2 First Condition

The first condition is the condensation between TEG-tethered dipyrromethane **6** and alkyl-tethered α,α'-diformyl-dipyrromethane **13** in the presence of *p*-toluenesulfonic acid as the acid catalyst and $Zn(OAc)_2 \cdot 2H_2O$ as a template and subsequently oxidized the condensation products in air (Scheme 3-2).[1a] This type of reaction procedure is particularly used to obtain asymmetrically substituted *β*-alkyl type porphyrins.[1]

This reaction resulted in the formation of the target zinc porphyrin **1**-Zn. But the isomer **2**-Zn was also obtained at the same time and the ^1H NMR spectrum of the product in $CDCl_3$ displayed signals ascribable to only the two species (Figure 3-1). The ratio of **1**-Zn and **2**-Zn (**2**/**1**) was 0.88 and the total yield of the porphyrins was 3.1%. This isomer **2**-Zn was obtained from the scrambling reaction during the condensation (Chapter 3-4) and could not be removed by any kinds of chromatography.

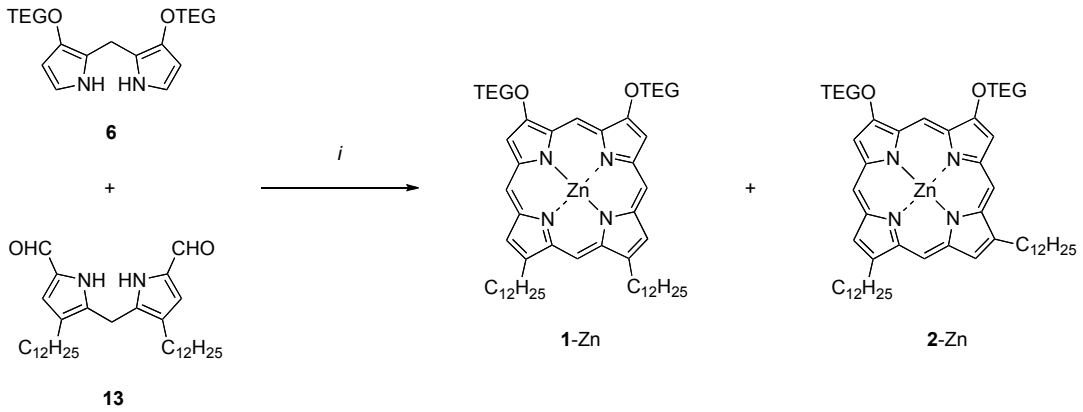

Scheme 3-2. Synthesis of amphiphilic porphyrin **1**-Zn under the first condition. (*i*) 1) *p*-TsOH, CH_2Cl_2, MeOH, r. t., 4 h.; 2) $Zn(OAc)_2$, r. t., 14 h, 3.1% (mixture, **2**-Zn / **1**-Zn = 0.88).

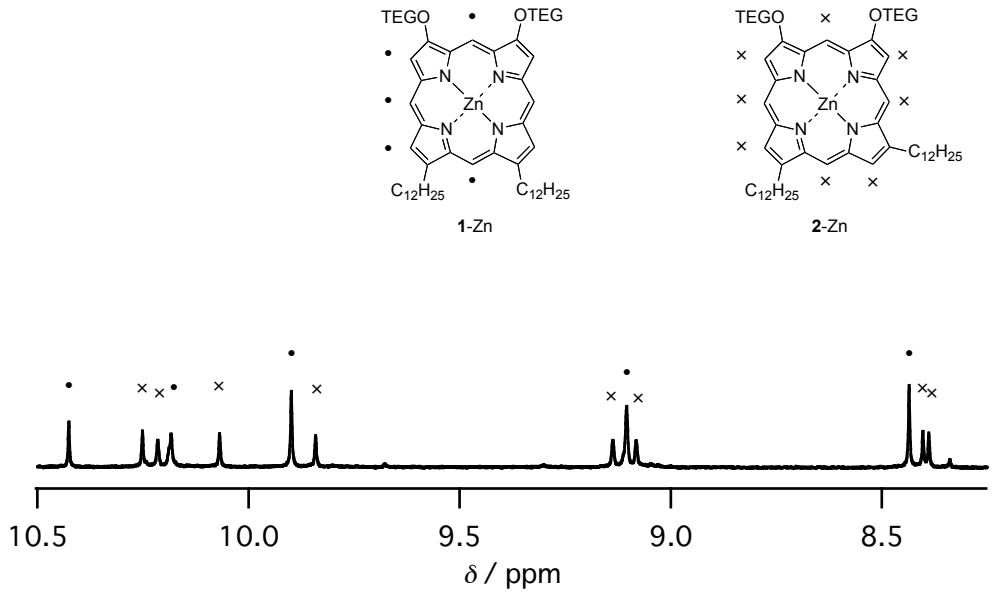

Figure 3-1. ^{1}H NMR spectrum of the product in $CDCl_3$. Porphyrin condensation was performed by the first condition.

3-3 Second Condition

For the second condition, I employed trifluoroacetic acid (TFA) as the catalyst for the condensation reaction between TEG-tethered dipyrromethane **6** and alkyl-tethered α,α'-diformyl-dipyrromethane **13** and subsequently oxidized the condensation products with *p*-chloranil (Scheme 3-3).[1c] These reagents are widely utilized for obtaining *meso*-aryl type porphyrins by 2 + 2 synthesis.[2]

With this condition, I obtained the target free-base porphyrin **1**-H_2 and the isomer **2**-H_2, whose isomeric ratio **2/1** was 7.9 with the total porphyrin yield of 1.9% (Figure 3-2). Strangely, the amount of the target porphyrin **1**-H_2 was much smaller than that of the isomer **2**-H_2 which was formed from the side reaction pathway during the condensation (Chapter 3-4). In these two reaction conditions to use α,α'-diformyl-dipyrromethane **13**, satisfactory isomeric ratios with good total yield of porphyrins could not be obtained.

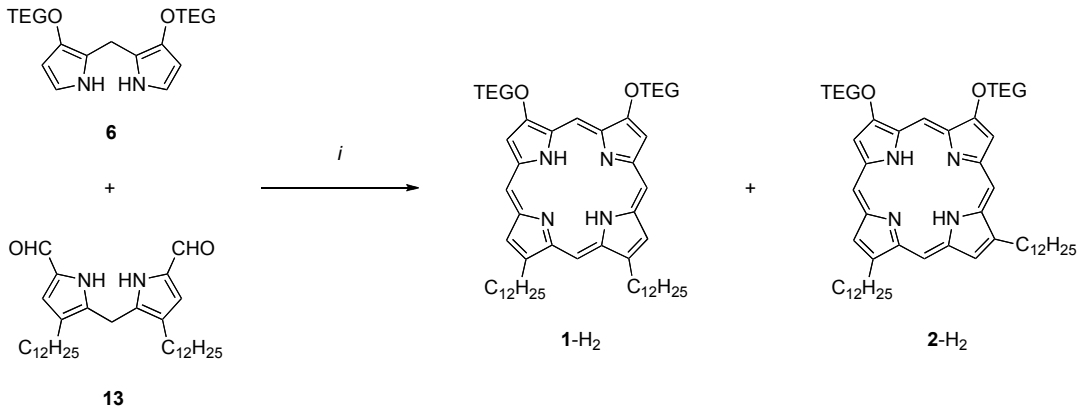

Scheme 3-3. Synthesis of amphiphilic porphyrin **1**-H_2 under the second condition. (*i*) 1) TFA, CH_2Cl_2, r. t., 21 h.; 2) *p*-chloranil, r. t., 2.5 h, 1.9% (mixture, **2**-H_2 / **1**-H_2 = 7.9).

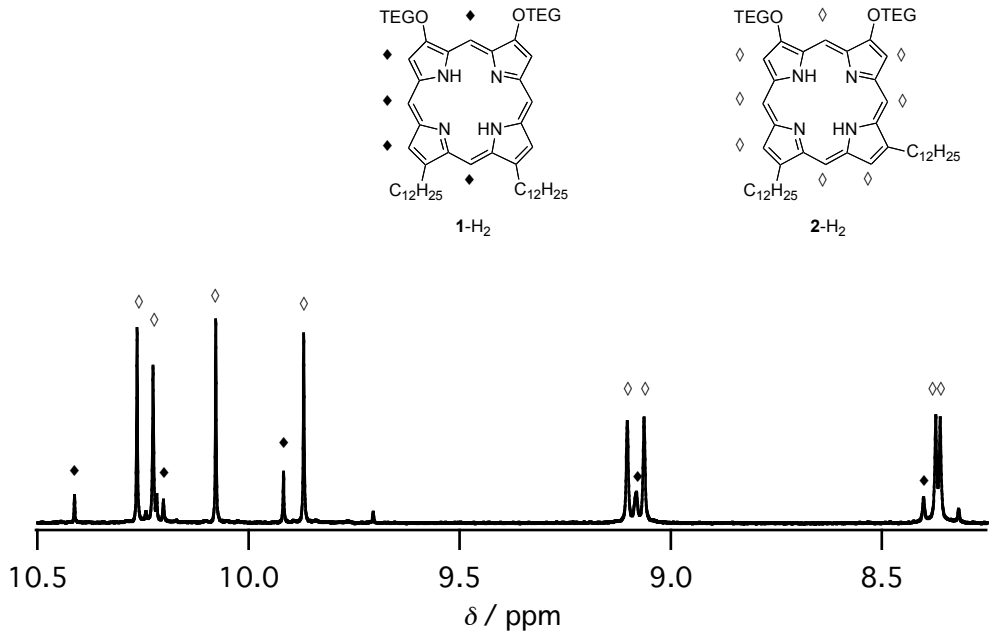

Figure 3-2. ^{1}H NMR spectrum of the product in $CDCl_3$. Porphyrin condensation was performed by the second condition.

3-4 Discussion of Scrambling Reaction

The exchange process frequently observed in polypyrrane condensation is proposed to occur by the acid-catalyzed fragmentation of a polypyrrane into pyrrolic and azafulvene components.[3] As illustrated in Scheme 3-4, recombination of them can form new polypyrranes and a resulting porphyrin isomer **2** that cannot be formed by direct condensation of the dipyrromethanes. Noteworthy, the obtainable isomers from this reaction should be only compound **2**, because this proposed reaction mechanism contains no polypyrrane to be able to be cyclized to porphyrinogen except the polypyrrane **2'**. Only considering the occurrence probabilities of the scrambling reaction, the ratio of **2**/**1** should not exceed 1. Close look at the reaction intermediates **1'** and **2'** to afford compounds **1** and **2**, respectively, reveals that the R_1 group of the intermediate **1'** attacks at the α'-position (5-position) of the TEG-tethered pyrrole to give the corresponding porphyrinogen. On the other hand, intermediate **2'** substitutes the α-position (2-position) of the alkyl-tethered pyrrole. The difference in the reactivity between the α- and α'-carbons of the β-mono-substituted pyrrole rings may cause the excessive yield of **2** over **1** under the conditions.

From this discussion, essentials to obtain the satisfactory isomeric ratios are (a) the choice of the R_1 groups at the alkyl-tethered dipyrromethane to selectively exchange α'-position of the TEG-tethered pyrrole and (b) the condensation in absence of Brønsted acids because a protonation reaction causes the formation of the transition species which is led to the isomeric intermediate **2'**. These two factors have been investigated in the third (Chapter 3-4) and fourth (Chapter 3-5) conditions.*

* After the defence for my Ph. D degree, another information of this porphyrin isomerization was obtained by 2D ROESY NMR spectroscopy. If you need it, this information can be ordered from the author (masafumi_oda_field_of_view@yahoo.co.jp).

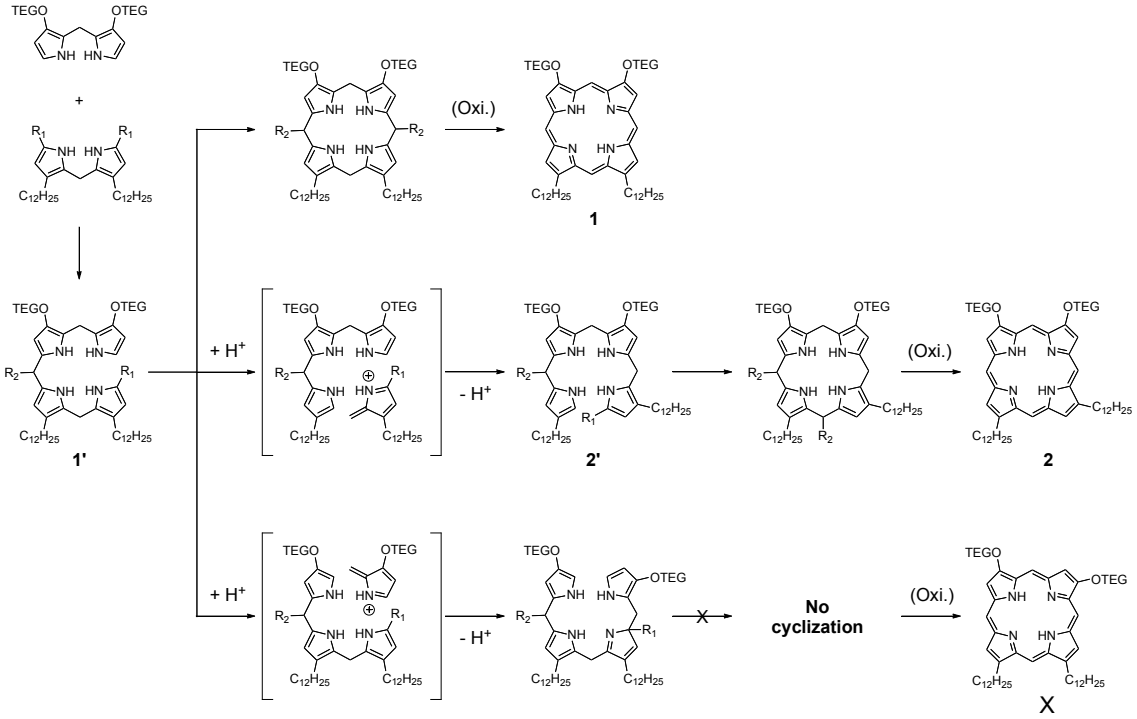

Scheme 3-4. A plausible reaction mechanism of the scrambling in the porphyrin condensation.

3-5 Third Condition

The formyl groups at the α,α'-positions of α,α'-diformyl-dipyrromethane **13** can be easily reduced to hydroxymethyl groups by sodium borohydride.[4b] The third condition was the condensation between TEG-tethered dipyrromethane **6** and alkyl-tethered α,α'-dihydroxymethyl-dipyrromethane **14** with acetic acid as the catalyst and the subsequent oxidation by *o*-chloranil (Scheme 3-5).[4] With this condition, the total yield of the porphyrins was 1.9% and the ratio of **2**/**1** was 6.0.

Furuta and Osuka *et al*. have reported that the scrambling problem was suppressed by using of hydroxymethyl groups-appended dipyrromethanes for condensation in the case of the syntheses of N-confused porphyrin.[4b] But in this case, the isomerization was not avoided in this condensation pathway.

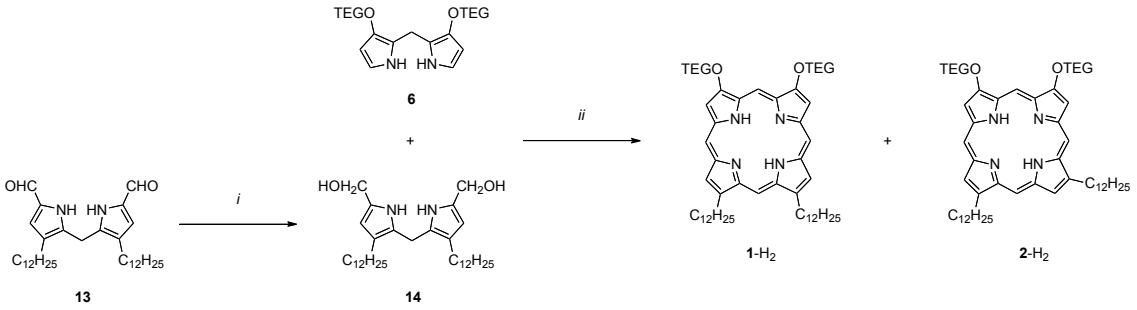

Scheme 3-5. Synthesis of amphiphilic porphyrin **1**-H_2 under the third condition. (*i*) $NaBH_4$, THF, MeOH, r. t., 3 h.; (*ii*) 1) AcOH, MeOH, r. t., 29 h.; 2) *o*-chloranil, r. t., 1.5 h, 1.9% (mixture, **2**-H_2 / **1**-H_2 = 6.0).

3-6 Fourth Condition

Recently, Lindsey *et al*. have reported a new method for the syntheses of asymmetrically *meso*-substituted porphyrins, where an imino-derivative of diformyl-dipyrromethane was employed.[5] The fourth condition is the modified condensation of the Lindsey's method, where a TEG-tethered dipyrromethane **6** and an alkyl-tethered α,α'-dipropylimino-dipyrromethane **15** are condensed in the presence of $Zn(OAc)_2 \cdot 2H_2O$ in refluxing toluene (Scheme 3-6). As a result of this reaction, much improved isomeric ratio **2/1** (= 0.18) was obtained and the total yield of porphyrins reached to 12%.

I investigated the temperature and solvent effects on the reaction (Table 3-1). At first, three solvents with almost similar dielectric constants (benzene: b. p. = 80 °C and ε_r = 2.3, toluene: b. p. = 111 °C and ε_r = 2.4, and xylene: b. p. = 138-145 °C and ε_r = 2.3-2.6) were employed at each boiling points to confirm the temperature effect on the condensation (entry 1, 2, and 3), and the lower reaction temperature afforded a better isomeric ratio of **2/1**. When the polarity of the solvents was varied, a less polar solvent afforded a better isomeric ratio **2/1** (entry 3, 4, 5, and 6).* The best result was achieved by the condensation in cyclohexane (b. p. = 81 °C, ε_r = 2.0), where the isomeric ratio of **2/1** reached to 0.05 and the total yield of porphyrins was 12% (Figure 3-4). In the proposed mechanism of the scrambling reaction (Chapter 3-4, Scheme 3-4), ionic intermediates or transition species would participate in the pathway, and they might be destabilized in less polar solvents. Therefore, less polar solvents such as cyclohexane can afford better isomeric ratios. Lower reaction temperature may also assist the better isomeric ratios by hampering pathways of the scrambling reactions.

* Only 1,2-dichloroethane showed deviation from the tendency. According to Scheme 3-4, the presence of H^+ promotes the scrambling reaction. Probably, because 1,2-dichloroethane contains a little amount of acid and it may cause a worse isomeric ratio **2**/**1** than EtOH.

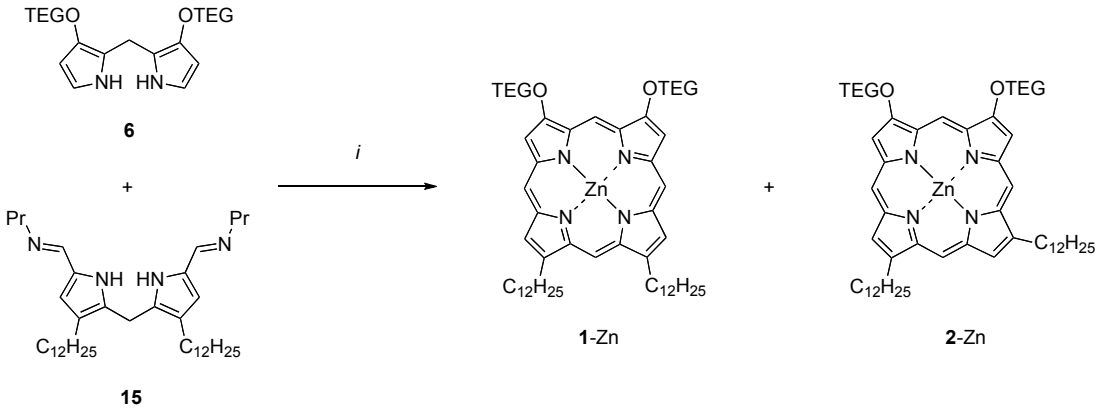

Scheme 3-6. Synthesis of amphiphilic porphyrin **1**-Zn under the fourth condition (entry 1). (*i*) $Zn(OAc)_2$, toluene, reflux, 4 h, 12% (mixture, **2**-Zn / **1**-Zn = 0.18).

Table 3-1. The total reaction yields of the porphyrin isomers and the isomeric ratios between **1**-Zn and **2**-Zn from the procedure in Scheme 3-6 (the fourth condition) at the concentration of the substrate with 10 mM.

entry	solvent	ε_r	b. p.	yield	**2**/**1**
1	toluene	2.4	111	12	0.18
2	xylene	2.3-2.6	138-145	14	0.65
3	benzene	2.3	80	8.0	0.10
4	EtOH	25	79	4.7	0.23
5	1,2-dichloroethane	10	84	2.1	0.72
6	cyclohexane	2.0	81	12	0.05

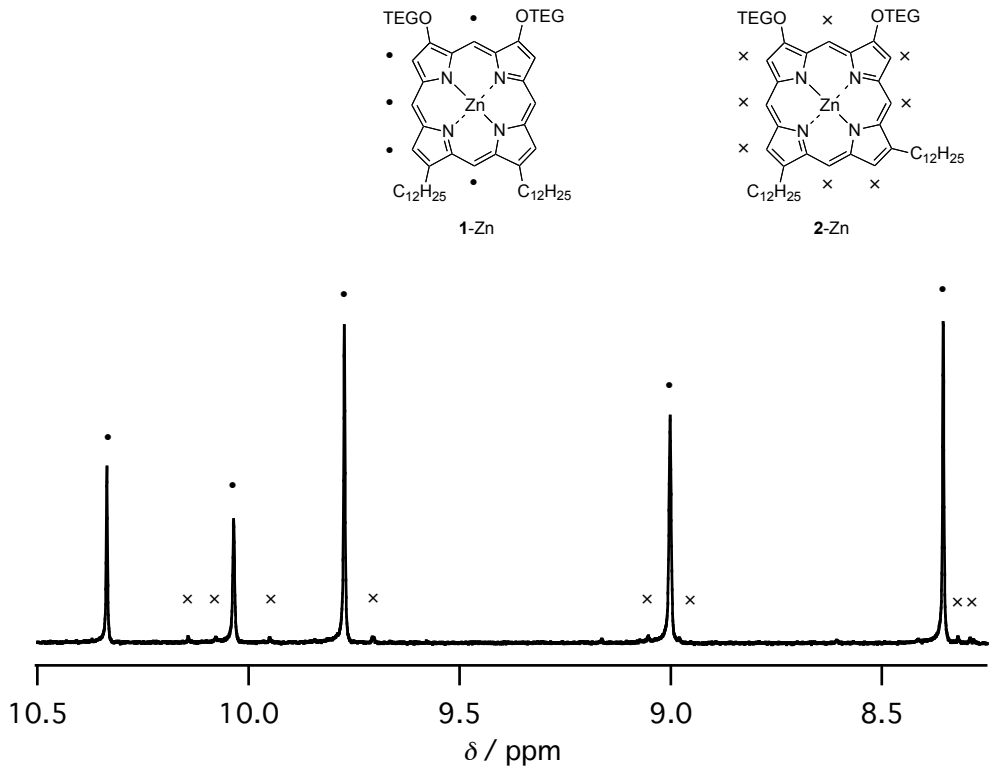

Figure 3-3. ^{1}H NMR spectrum of the product in $CDCl_3$. Porphyrin condensation was performed by the fourth condition (entry 6).

3-7 Preparative Syntheses of Target Porphyrin Complexes

For the preparative synthesis, the condensation was done under the fourth condition (entry 6) with 0.24 mmol each of the dipyrromethane derivatives, and 44.8 mg of the porphyrin mixture was obtained in 18% yield with **2**/**1** isomeric ratio of 0.03 (Scheme 3-7). The isolation of the target porphyrin **1**-Zn from the isomeric mixture was accomplished by repeated recrystallizations from the solution in CH_2Cl_2-MeOH mixed solvent. As a result, the isomeric mixture of 44.8 mg afforded 22.5 mg of the target **1**-Zn to be pure at NMR level (Figure 3-4). The characterization of the target porphyrin has been done by ^{1}H and ^{13}C NMR spectroscopies and HR FAB-MS spectrometry.

The central zinc atom was demetallated under the acidic condition with TFA in CH_2Cl_2 and the freebase porphyrin **1**-H_2 was obtained in 98% yield. The insertion of copper was carried out by refluxing the solution of **1**-H_2 in the presence of $Cu(OAc)_2 \cdot H_2O$ to give the target compound **1**-Cu quantitatively.

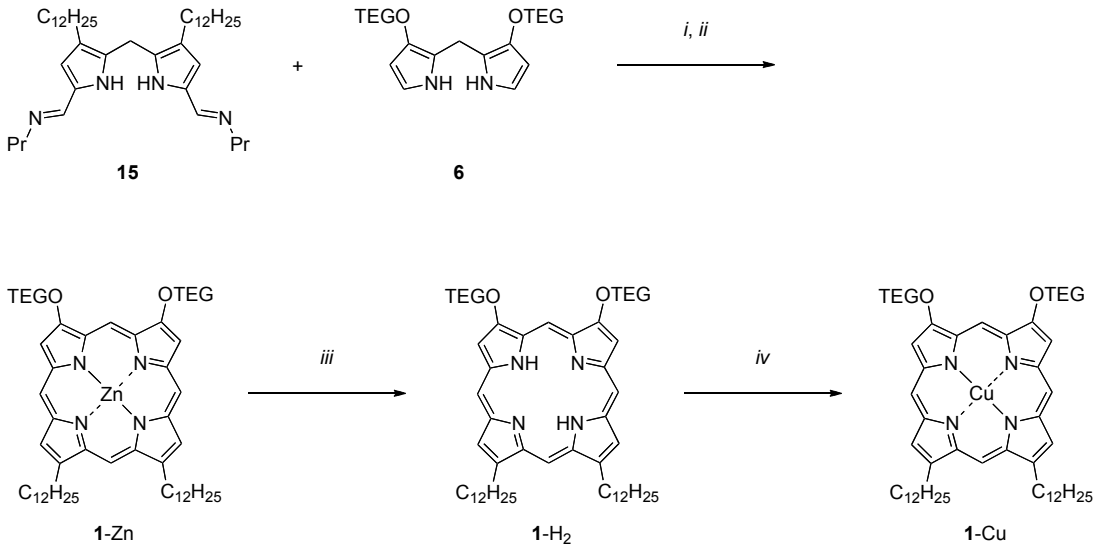

Scheme 3-7. Preparative synthesis of amphiphilic porphyrin **1**-M. (*i*) $Zn(OAc)_2$, cyclohexane, reflux, 26 h, 18% (mixture, **2**-Zn / **1**-Zn = 0.03).; (*ii*) recrystallization, CH_2Cl_2–MeOH, 50%.; (*iii*) TFA, CH_2Cl_2, 0 ºC, 6 h, 98%.; (*iv*) $Cu(OAc)_2$, CH_2Cl_2, MeOH, reflux, 1 h, quant.

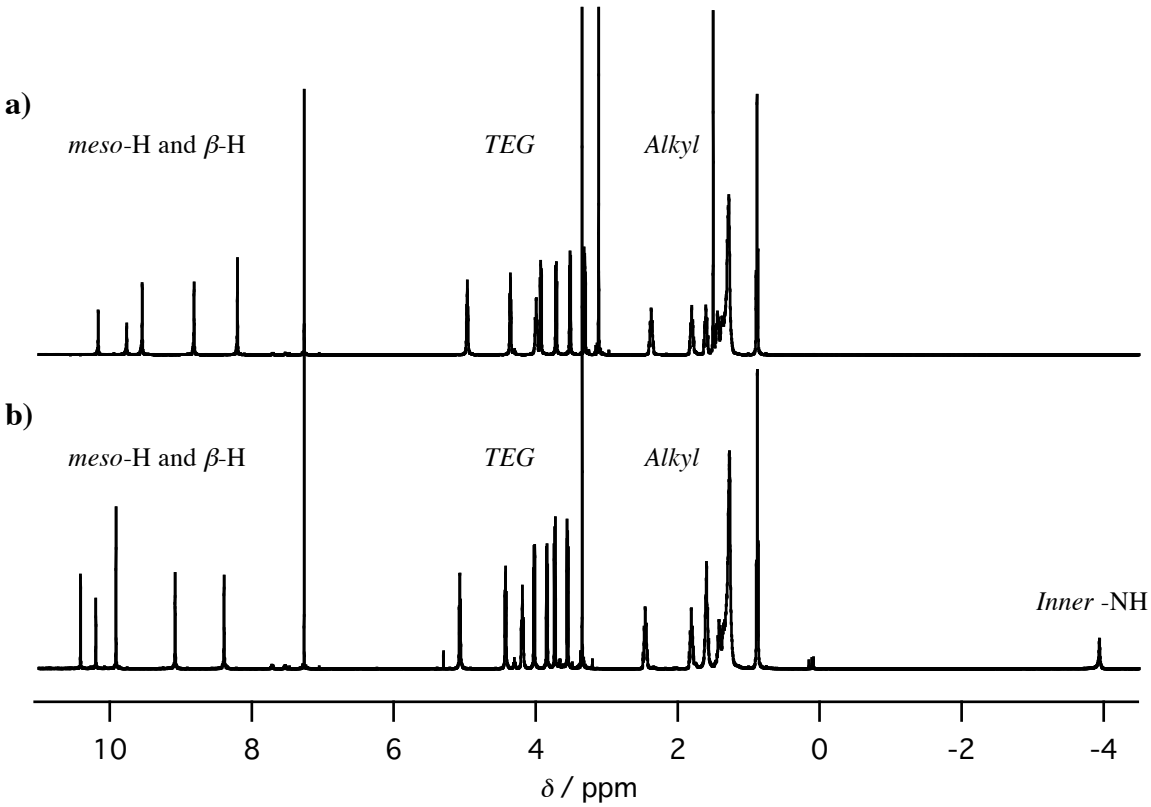

Figure 3-4. ^1H NMR spectra of (a) **1**-Zn and (b) **1**-H_2 in $CDCl_3$.

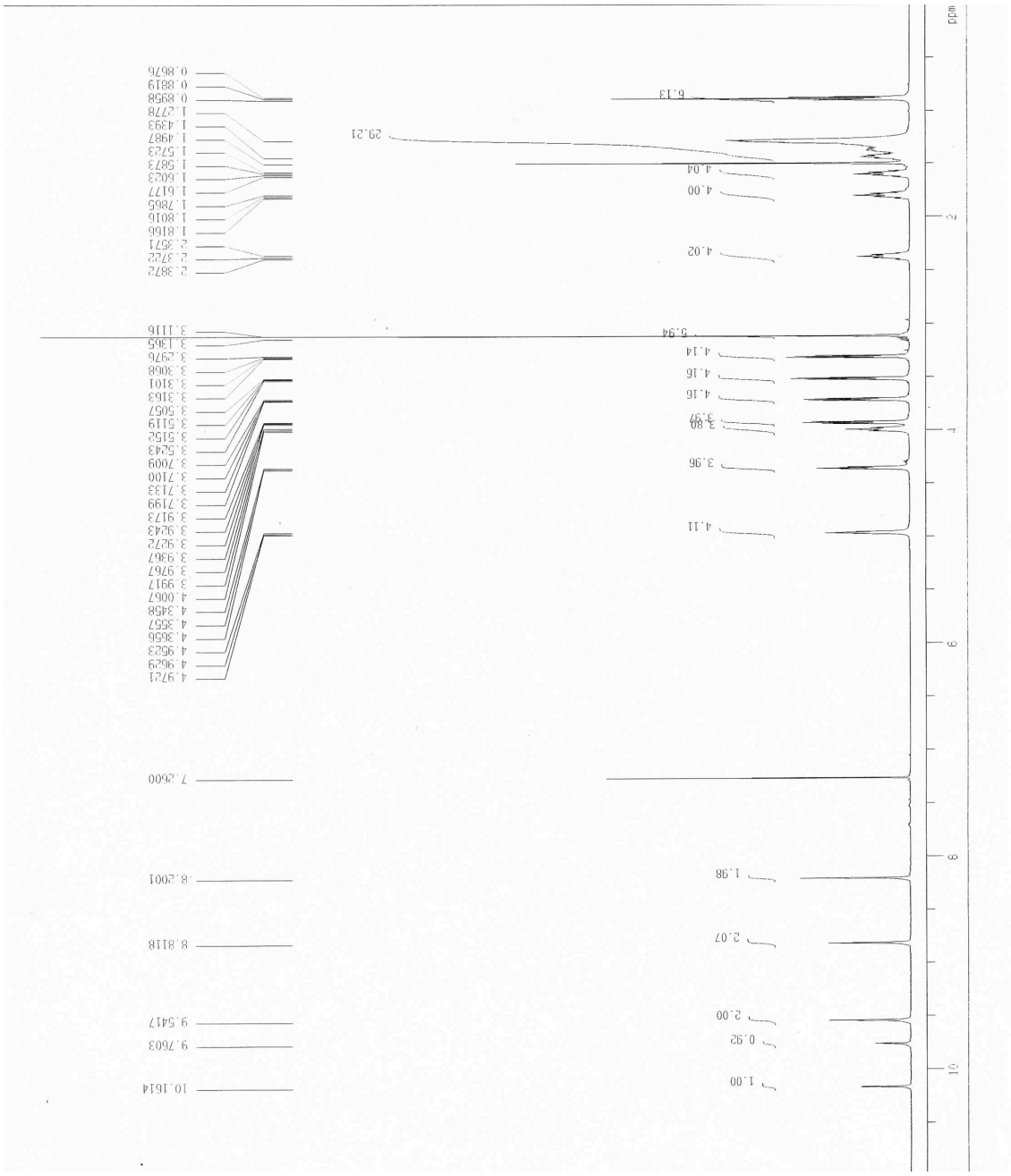

Figure 3-5. ^{1}H NMR spectrum of **1**-Zn in $CDCl_3$.

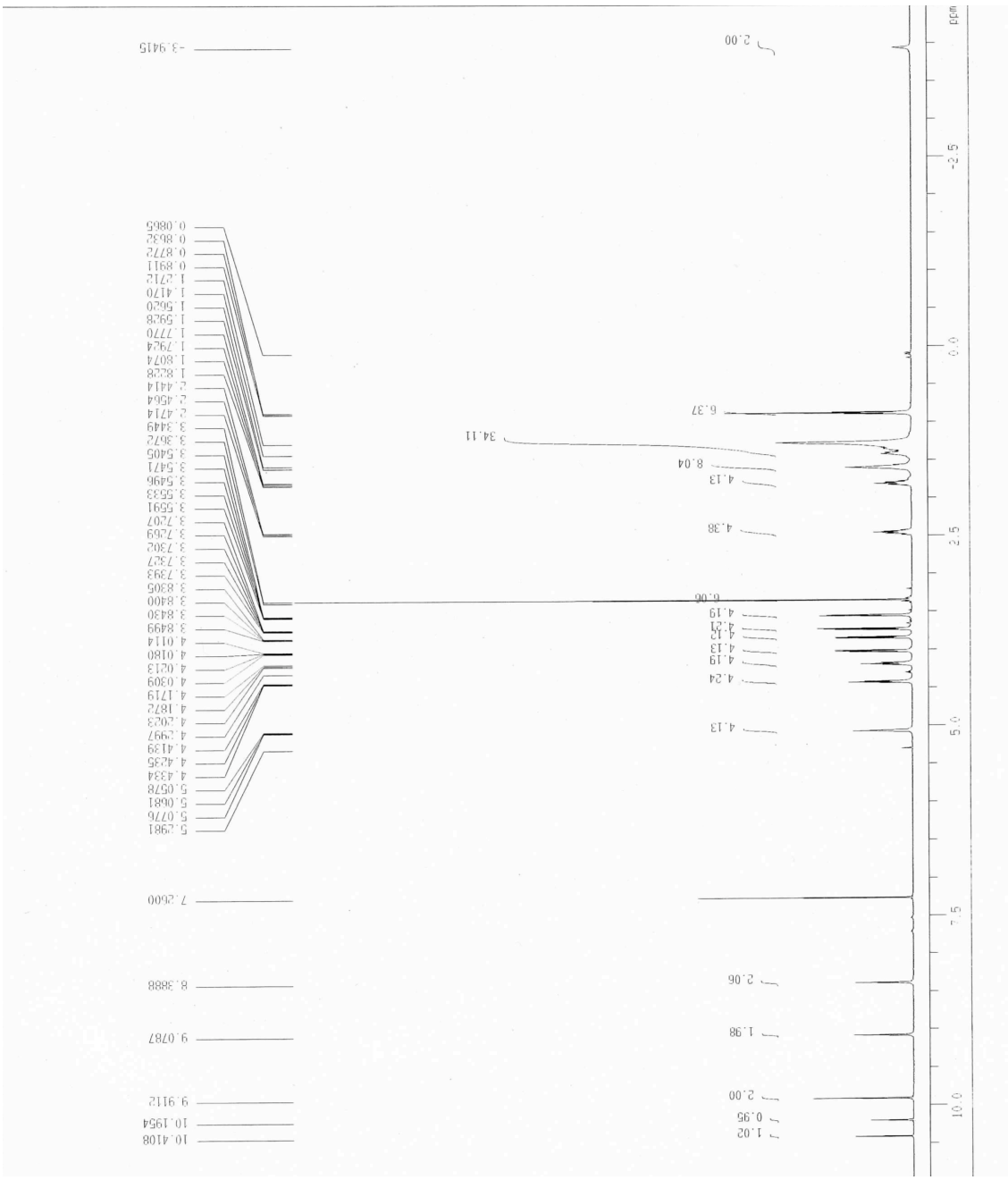

Figure 3-6. ^{1}H NMR spectrum of **1**-H_2 in $CDCl_3$.

3-8 Conclusion

I have succeeded in the synthesis of highly planar and amphiphilic *β*-alkylporphyrin and investigated the temperature and solvent effects on the condensation reaction for the porphyrin synthesis. Suppressing the scrambling problem is of great importance for synthesizing asymmetric porphyrins, and thus the proposed solution here will contribute to the future development of porphyrin chemistry and the material application.

3-9 Experimental Section

General. THF was freshly distilled over benzophenone ketyl under Ar before use. Dichloromethane was distilled over calcium hydride under Ar. Methanol was distilled under Ar before use. Triethylamine, zinc(II) acetate dihydrate and copper(II) acetate monohydrate were purchased from Kanto Chemicals. *p*-Toluenesulfonic acid monohydrate was obtained from Wako Pure Chemical Industries. Sodium borohydride, *p*-chloranil, *o*-chloranil, trifluoroacetic acid and glacial acetic acid were purchased from Aldrich. Sodium sulfate and sodium bicarbonate were obtained from Nacalai Tesque. Column chromatography was performed on the bench top, using silica gel (Wakogel C–300HG). All deuterated solvents for NMR measurement were used as received from Cambridge Isotope Laboratories, Inc.

^{1}H and ^{13}C NMR spectra were recorded on a JEOL model JNM–LA400 or JNM-LA500 NMR spectrometer, where chemical shifts (δ in ppm) were determined with a residual proton or the carbon-13 signals of the solvent as standard. All *J* values are reported in Hertz. Matrix–assisted laser desorption ionization time–of–flight mass (MALDI–TOF MS) spectroscopic data were obtained with an Applied Biosystems BioSpectrometry model Voyager–DE–STR spectrometer in reflector or linear mode. Samples were prepared as micromolar solutions in dichloromethane or THF, and dithranol (Aldrich) was utilized as the matrix. Fast atom bombardment mass spectra (FAB-MS) and high-resolution mass spectra were recorded on a JEOL model JMS-700 spectrometer in the positive ion mode with a xenon primary atom beam with 3-nitrobenzylalcohol matrix. Electronic absorption spectra were recorded on a JASCO model V–570 spectrophotometer using a quartz cell of 1–cm and 1–mm path length on equipped with a temperature controller.

(A) First Condition. To a predried **6** (29.5 mg, 62.7 μmol) and **13** (33.8 mg, 62.7 μmol) in a 50 mL round bottom flask were injected dry dichloromethane (6.3 mL) and dry methanol (0.63 mL) under Ar. Dry methanol (0.63 mL) solution of *p*-toluenesulfonic acid monohydrate (36.9 mg, 194 μmol) was added dropwise at room temperature and the reaction mixture was stirred for 4 h. Saturated solution of zinc(II) acetate dihydrate in methanol (0.65 mL) was added dropwise and the mixture was stirred under air for 14 h. Sat. sodium bicarbonate (aq) (13 mL) was added and the mixture was extracted with dichloromethane (15 mL, 3 times). The combined organic phase was dried over anhydrous sodium sulfate, filtered, and evaporated *in vacuo*. The residue was purified by column chromatography on silica gel eluted with chloroform-acetone (10:1), and the third fraction was collected and the solvent was

evaporated under vacuum to give the mixture (2.0 mg, 1.9 μmol) of the product **1**-Zn and the isomer **2**-Zn as a reddish purple solid. The ratio of **1**-Zn and **2**-Zn (**2**/**1**) was 0.88 determined by ^{1}H NMR and the total yield was 3.1%.

(B) Second Condition. To a predried **6** (26.0 mg, 55.3 μmol) and **13** (29.8 mg, 55.3 μmol) in a 50 mL round bottom flask were injected dry dichloromethane (18.4 mL) under Ar. Trifluoroacetic acid (1.0 μL, 14 μmol) was added and the reaction mixture was stirred at room temperature for 5 h. Additional trifluoroacetic acid (7.0 μL, 96 μmol) was added and the mixture was stirred for further 16 h. *p*-Chloranil (13.6 mg, 55.3 μmol) was added and the mixture was stirred for 2.5 h. Triethylamine (16 μL, 0.11 mmol) was added and the solvent was evaporated *in vacuo*. The residue was purified by column chromatography on silica gel eluted with ethyl acetate, and the second fraction was collected. The solvent was evaporated under vacuum to afford the mixture (1.0 mg, 1.0 μmol) of the product **1**-H_2 and the isomer **2**-H_2 as a reddish purple solid. The ratio of **1**-H_2 and **2**-H_2 (**2**/**1**) was 7.9 and the total yield was 1.9%.

(C) Third Condition. To a predried **13** (15.0 mg, 27.8 μmol) in a 50 mL round bottom flask were injected dry THF (1.6 mL) and dry methanol (0.4 mL) under Ar. Sodium borohydride (52.6 mg, 1.39 mmol) was added and the reaction mixture was stirred at room temperature for 3 h. Water (5 mL) was added and the mixture was extracted with dichloromethane (10 mL, 3 times). The combined organic phase was washed with brine, dried over anhydrous sodium sulfate, filtered, and evaporated *in vacuo* to afford 3,7-didodecyl-1,9-bis(hydroxymethyl)dipyrromethane **14**. The obtained **14** was used immediately without characterization. To a predried **6** (13.1 mg, 27.8 μmol) and the obtained **14** in a 50 mL round bottom flask were injected dry

methanol (9.3 mL) under Ar. Glacial acetic acid (19 μL, 330 μmol) was added and the reaction mixture was stirred at room temperature for 29 h. *o*-Chloranil (20.5 mg, 83.4 μmol) was added and the mixture was stirred for further 1.5 h. Sat. sodium bicarbonate (aq) (9 mL) was added and the mixture was extracted with dichloromethane (15 mL, 3 times). The combined organic phase was dried over anhydrous sodium sulfate, filtered, and evaporated *in vacuo*. The residue was purified by column chromatography on silica gel eluted with ethyl acetate-hexane, whose ratio was changed from 10:1 to 10:0, and the second fraction was collected and the solvent was evaporated under vacuum to afford the mixture (0.5 mg, 0.5 μmol) of the product **1**-H_2 and the isomer **2**-H_2 as a reddish purple solid. The ratio of **1**-H_2 and **2**-H_2 (**2**/**1**) was 6.0 and the total yield was 1.9%.

(D-1) Fourth Condition. A solution of **6** (25.2 mg, 53.6 μmol) and **15** (33.0 mg, 53.1 μmol) in toluene (5.4 mL) was treated with zinc(II) acetate dihydrate (0.1175 g, 535 μmol) under reflux for 4 h without deaeration. The solvent was removed *in vacuo*, and the residue was purified by column chromatography on silica gel eluted with ethyl acetate-hexane whose ratio was gradually changed from 10:1 to 10:0. The third fraction was collected and the solvent was evaporated under vacuum to afford the mixture (6.6 mg, 6.4 μmol) of the product **1**-Zn and the isomer **2**-Zn as a reddish purple solid. The ratio of **1**-Zn and **2**-Zn (**2**/**1**) was 0.18 and the total yield was 12%.

(D-2). As following the procedure **(D-1)**, benzene (2.8 mL) was used as a reaction solvent and the product mixture (2.3 mg) was obtained in 8.0% yield and the ratio **2**/**1** was 0.10.

(D-3). As following the procedure **(D-1)**, xylene (4.8 mL) was used as a reaction solvent and the product mixture (6.7 mg) was obtained in 14% yield and the ratio **2**/**1**

was 0.65.

(D-4). As following the procedure **(D-1)**, ethanol (5.6 mL) was used as a reaction solvent and the product mixture (2.7 mg) was obtained in 4.7% yield and the ratio **2**/**1** was 0.23.

(D-5). As following the procedure **(D-1)**, 1,2-dichloroethane (3.7 mL) was used as a reaction solvent and the product mixture (0.8 mg) was obtained in 2.1% yield and the ratio **2**/**1** was 0.72.

(D-6). As following the procedure **(D-1)**, cyclohexane (3.2 mL) was used as a reaction solvent and the product mixture (4.0 mg) was obtained in 12% yield and the ratio **2**/**1** was 0.05.

Preparative synthesis of Porphyrin (1-Zn). A solution of **6** (0.1141 g, 0.2425 mmol) and **15** (0.1512g, 0.2435 mmol) in cyclohexane (24.3 mL) was treated with zinc(II) acetate dihydrate (0.5350 g, 2.437 mmol) under reflux for 26 h without deaeration. The solvent was removed *in vacuo* and the residue was purified by column chromatography on silica gel eluted with ethyl acetate-hexane, whose ratio was gradated from 10:1 to 10:0. The first fraction was collected and the solvent was evaporated under vacuum to afford the mixture (44.8 mg, 43.3 μmol) of the product **1**-Zn and the isomer **2**-Zn as a reddish purple solid. The ratio of **1**-Zn and **2**-Zn (**2**/**1**) was 0.03 and the total yield was 18%. Two times of recrystallization from dichloromethane–methanol afforded the pure product **1**-Zn (22.5 mg, 21.7 μmol) as a reddish purple solid. ^{1}H NMR ($CDCl_3$): δ 10.16 (s, 1H), 9.76 (s, 1H), 9.54 (s, 2H), 8.81 (s, 2H), 8.20 (s, 2H), 4.96 (t, 4H, J = 5.0 Hz), 4.36 (t, 4H, J = 5.0 Hz), 3.99 (t, 4H, J = 7.5 Hz), 3.94-3.92 (m, 4H), 3.72-3.70 (m, 4H), 3.52-3.51 (m, 4H), 3.32-3.30 (m, 4H), 3.11 (s, 6H), 2.39-2.36 (m, 4H), 1.82-1.79 (m, 4H), 1.62-1.59 (m, 4H), 1.44-1.28

(m, 28H), 0.88 (t, 6H, J = 7.1 Hz). ^{13}C NMR ($CDCl_3$): δ 162.30, 147.99, 147.46, 146.91, 145.93, 140.57, 127.91, 104.74, 103.16, 97.62, 94.47, 71.84, 71.27, 71.20, 70.88, 70.55, 70.12, 58.90, 32.09, 32.02, 30.30, 30.04, 29.99, 29.99, 29.94, 29.86, 29.55, 28.19, 22.84, 14.26. UV/vis (THF): λ_{max} [nm] (ε [$M^{-1}cm^{-1}$]) 325 (23600), 405 (297000), 526 (10900), 540 (13200), 561 (19100), 581 (21900). HRMS: m/z = 1032.5854 (calcd. for $C_{58}H_{88}N_4O_8Zn$ $[M]^+$ = 1032.5894).

Demetallation of a Zinc Porphyrin (1-H_2). To a solution of **1**-Zn (11.4 mg, 11.0 μmol) in dichloromethane (2.2 mL) was added trifluoroacetic acid (0.11 mL, 1.5 mmol) dropwise at 0 ºC under Ar and stirred at the temperature for 6 h. The reaction mixture was carefully poured into sat. sodium bicarbonate (aq) (20 mL) at 0 ºC and stirred at room temperature for 30 min. The mixture was extracted with dichloromethane (20 mL, 3 times), and the combined organic phase was dried over anhydrous sodium sulfate and evaporated *in vacuo*. The residue was purified by column chromatography on silica gel eluted with dichloromethane-methanol, whose ratio was gradated from 10:1 to 10:0. The first fraction was collected and the solvent was evaporated under vacuum to afford the product **1**-H_2 (10.5 mg, 10.8 μmol) as a reddish purple solid in 98% yield. ^{1}H NMR ($CDCl_3$): δ 10.41 (s, 1H), 10.20 (s, 1H), 9.91(s, 2H), 9.08 (s, 2H), 8.39 (s, 2H), 5.07 (t, 4H, J = 5.0 Hz), 4.42 (t, 4H, J = 4.9 Hz), 4.19 (t, 4H, J = 7.6 Hz), 4.03-4.01 (m, 4H), 3.85-3.83 (m, 4H), 3.74-3.72 (m, 4H), 3.56-3.54 (m, 4H), 3.34 (s, 6H), 2.46 (t, 4H, J = 7.5 Hz), 1.81 (t, 4H, J = 7.6 Hz), 1.59 (bs, 4H), 1.42-1.27 (m, 28H), 0.88 (t, 6H, J = 7.0 Hz), -3.94 (bs, 2H). UV/vis (THF): λ_{max} [nm] (ε [$M^{-1}cm^{-1}$]) 397 (144000), 496 (13400), 528 (13300), 568 (6930), 622 (9330). HRMS: m/z = 971.6832 (calcd. for $C_{58}H_{91}N_4O_8$ $[M+H]^+$ = 971.6837).

Cu (II) complex (1-Cu). A solution of **1**-H_2 (27.8 mg, 28.6 μmol) in

dichloromethane (1.7 mL) was added sat. copper(II) acetate monohydrate in methanol (3.4 mL) under Ar and refluxed for 1 h. The reaction mixture was poured into water (10 mL), extracted with dichloromethane (12 mL, 3 times). The combined organic phase was dried over anhydrous sodium sulfate and evaporated *in vacuo*. The residue was purified by column chromatography on silica gel eluted with dichloromethane-methanol, whose ratio was gradually changed from 10:1 to 10:0. The first fraction was collected and the solvent was evaporated under vacuum to give the product **1**-Cu (30.6 mg, 29.6 μmol) as a reddish purple solid in quantitative yield. UV/vis (THF): λ_{max} [nm] (ε [$M^{-1}cm^{-1}$]) 321 (15600), 398 (220000), 516 (7260), 529 (8930), 552 (16200), 570 (16700). HRMS: *m/z* = 1032.5940 (calcd. for $C_{58}H_{89}CuN_4O_8$ $[M+H]^+$ = 1032.5976).

3-10 References

1. (a) Omote, M.; Ando, A.; Takagi, T.; Koyama, M.; Kumadaki, I. *Tetrahedron* **1996**, *52*, 13961-13970. (b) Lash, T. D.; Chen, S. *Tetrahedron* **2005**, *61*, 11577-11600. (c) Juillard, S.; Simonneaux, G. *Synlett* **2006**, 2818-2820. (d) Uno, H.; Nakamoto, K.; Kuroki, K.; Fujimoto, A.; Ono, N. *Chem. Eur. J.* **2007**, *13*, 5773-5784.

2. Recent reviews: (a) Lindsey, J. S. *Acc. Chem. Res.* **2009**, ASAP (DOI: 10.1021/ar900212t). (b) Shanmugathasan, S.; Edwards, C.; Boyle, R. W. *Tetrahedron* **2000**, *56*, 1025-1046.

3. Littler, B. J.; Ciringh, Y.; Lindsey, J. S. *J. Org. Chem.* **1999**, *64*, 2864-2872.

4. (a) Maruyama, K.; Nagata, T.; Ono, N.; Osuka, A. *Bull. Chem. Soc. Jpn.* **1989**, *62*, 3167-3170. (b) Maeda, H.; Osuka, A.; Ishikawa, Y.; Aritome, I.; Hisaeda, Y.; Furuta, H. *Org. Lett.* **2003**, *5*, 1293-1296.

5. Taniguchi, M.; Balakumar, A.; Fan, D.; McDowell, B. E.; Lindsey, J. S. *J. Porphyrins Phthalocyanines* **2005**, *9*, 554-574.

Chapter 4.

Supramolecular Integration of Porphyrins in Polar Solvents

Published in *Tetrahedron Lett*. **2009**, *50*, 7137–7140.

Masafumi Oda, Tomoya Ishizuka, Shigeo Arai, Atsushi Takano, and Donglin Jiang

4-1 UV-Vis Spectral Changes in the Process of Self-Assembly of H_2- and Cu-Porphyrins

The supramolecular integration of the obtained porphyrins **1**-H_2 and **1**-Cu has been examined under several different conditions by employing the amphiphilic properties of the porphyrins. The UV-Vis spectral changes were observed on adding H_2O to the solution of the freebase **1**-H_2 in THF at the concentration of 1.1×10^{-4} M (Figure 4-1(a)). The Soret absorption band of **1**-H_2 shows red shift by 42 nm. Similar behaviors were observed for the absorption experiments of **1**-H_2 on cooling the hot MeOH solution (1.2×10^{-4} M). On the other hand, when H_2O was added to the solution of **1**-Cu in THF at the concentration of 4.9×10^{-5} M, the Soret absorption of **1**-Cu at 397 nm displayed clear blue shifts with a peak (λ_{max}) at 392 nm in THF-H_2O = 1:9 mixed solvent. In general, Kasha's exciton theory tells that a blue shift of the optical absorption indicates face-to-face H-aggregation of the chromophores.[1] In contrast to the changes in THF-H_2O experiments of **1**-Cu, the Soret absorption of **1**-Cu exhibits only decrease of the absorbance and no wavelength shifts at the experiment on cooling of the hot MeOH solution. This result may be caused by the low solubility of **1**-Cu in hot MeOH and the oligomeric aggregates cannot be detected in the spectra due that precipitated.

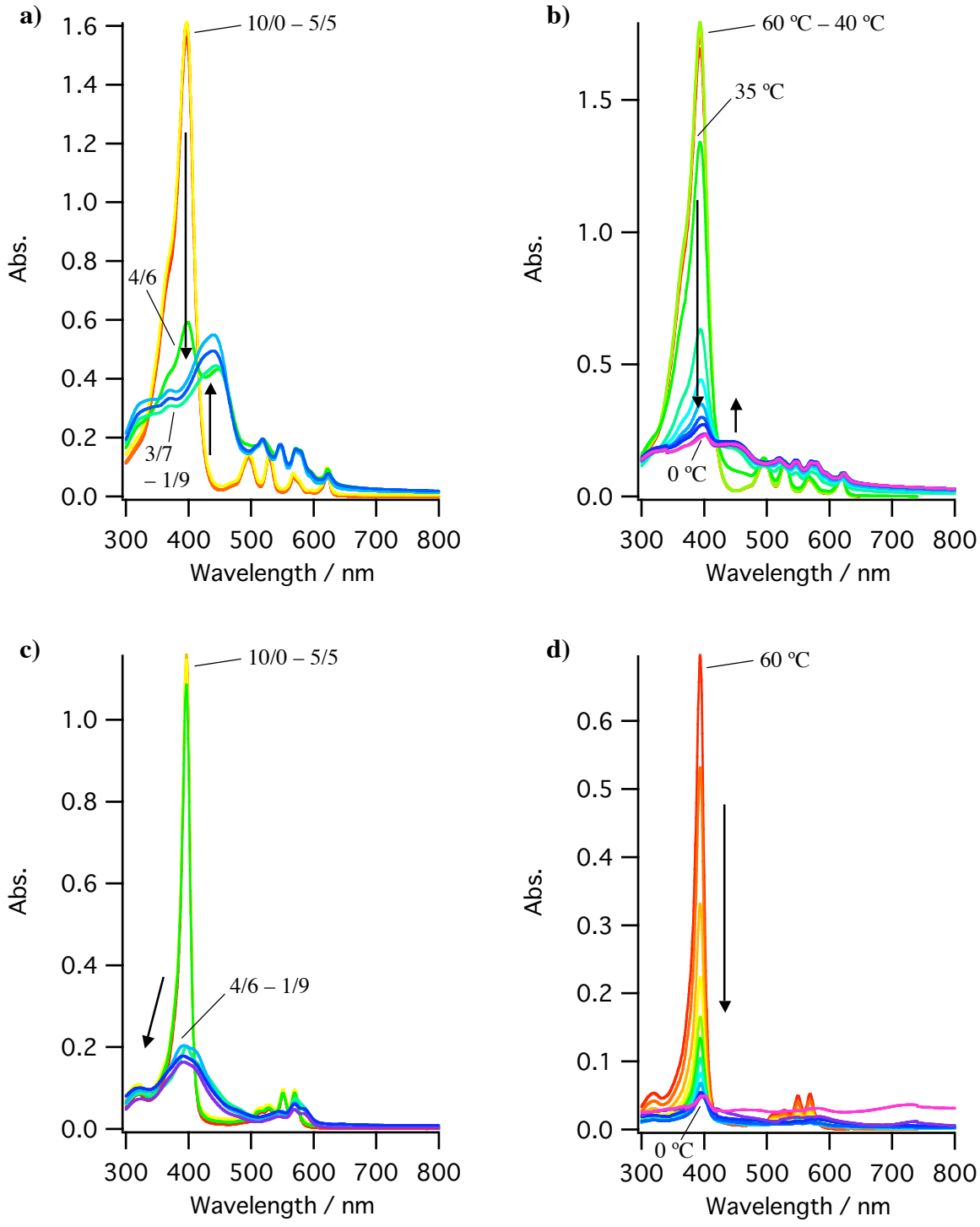

Figure 4-1. UV-Vis spectral changes of **1**-H_2 in (a) THF-H_2O mixed solvent with different ratios (v/v, [**1**-H_2] = 1.06 × 10^{-4} M) and (b) MeOH on cooling from 60 to 0 ºC ([**1**-H_2] = 1.18 × 10^{-4} M) and the spectral changes of **1**-Cu in (c) THF-H_2O mixed solvent with different ratios (v/v, [**1**-Cu] = 4.94 × 10^{-5} M) and (d) MeOH on cooling from 60 ºC to 0 ºC ([**1**-Cu] = 3.92 × 10^{-5} M).

4-2 SEM and TEM Observations of H_2- and Cu-Porphyrins Aggregates

The shapes of the nanostructures of the integrated porphyrin have been observed by scanning and transmission electron microscopies (SEM and TEM) (Figure 4-2, 4-3). When the suspension of freebase porphyrin **1**-H_2 precipitated from the hot MeOH solution was casted on an HOPG substrate, SEM observation revealed fiber-like structures with diameters between 75 and 550 nm and lengths of over 25 μm (Figure 4-2 c and d). The TEM images of the same sample of **1**-H_2 displayed that the rod structure consisted of the bundles of narrower wires with the diameter of 25 nm (Figure 4-3 c and d). Precipitate of **1**-H_2 from THF-H_2O also showed 1D-rod structures (Figure 4-2 a and b, 4-3 a and b). The precipitate of **1**-Cu obtained from THF-H_2O showed short rod-like structures with the diameter of *ca*. 11 nm and the length in the range of 140—310 nm as estimated by the SEM and TEM observations (Figure 4-2 e and f, 4-3 e and f). The SEM image of the precipitate of **1**-Cu obtained from a hot MeOH solution afforded a helical ribbon-structure without chiral selectivity (Figure 4-2 g and h).

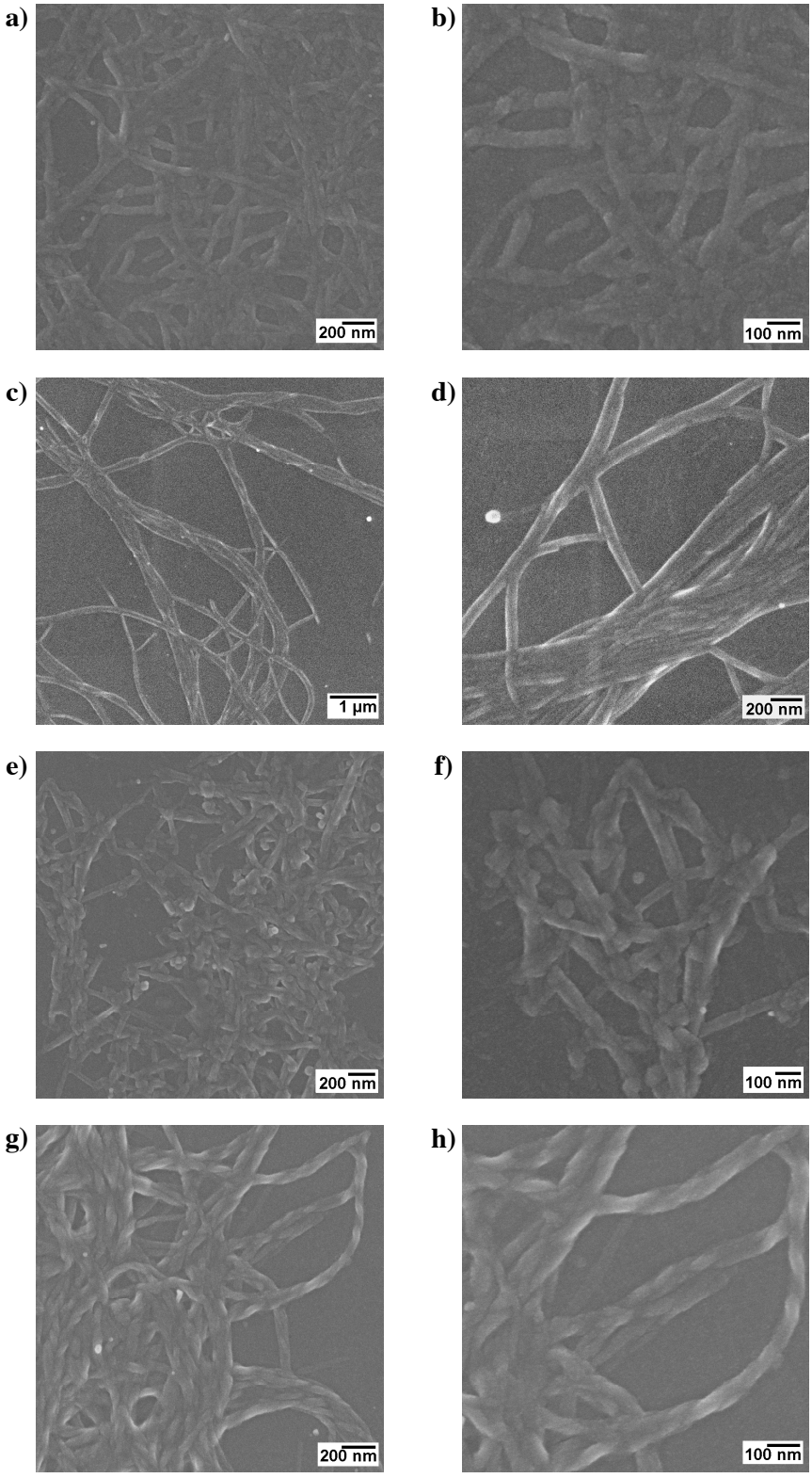

Figure 4-2. FE-SEM images of the precipitates of **1**-H_2 obtained from a) & b) THF-H_2O, c) & d) a hot MeOH solution and the images of **1**-Cu from e) & f) THF-H_2O, g) & h) a hot MeOH solution.

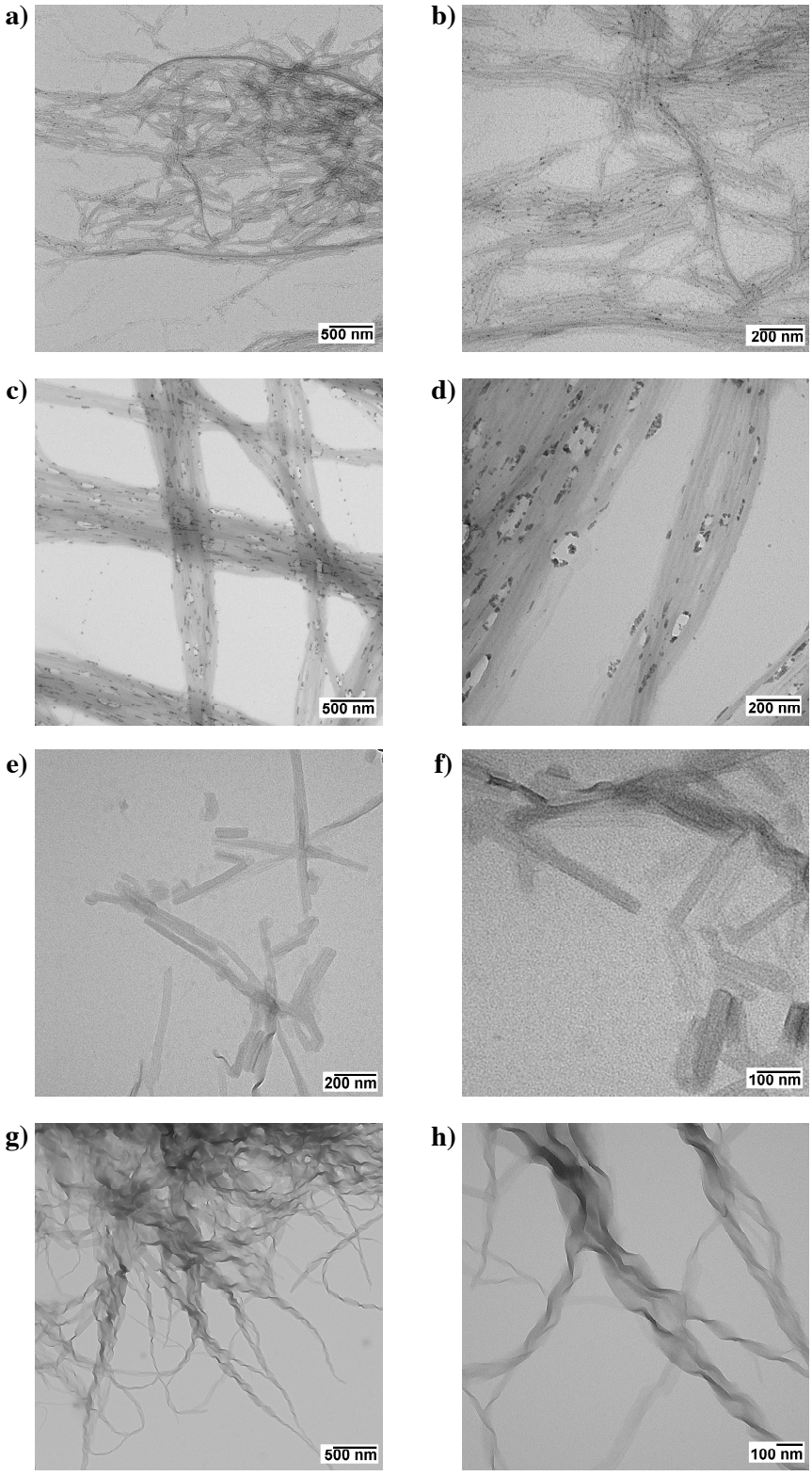

Figure 4-3. TEM images of the precipitates of **1**-H_2 obtained from a) & b) THF-H_2O, c) & d) a hot MeOH solution and the images of **1**-Cu from e) & f) THF-H_2O, g) & h) a hot MeOH solution.

4-3 XRD Analyses of H_2- and Cu-Porphyrins Aggregates

The XRD analysis of the precipitate of **1**-Cu from THF-H_2O solution has revealed that the molecules are packed in a *monoclinic* unit cell with the dimensions of a = 67.71(4), b = 3.546(3) and c = 24.62(2) Å and b = 96.72(7)° and the π-stacked 1-D chains are aligned to the b-axis with the π-stacking distance of 3.55 Å (Figure 4-4, Table 4-1). On the basis of an optimized structure of **1** (Figure 4-5), the observed cell parameters a and c can be assumed twice as large as the molecular length between the paraffinic and the TEG ends and the molecular width, respectively (Figure 4-6). Despite the clearly distinctive appearance with the SEM and TEM observations, the precipitate of **1**-Cu obtained from a hot MeOH solution displayed an almost identical XRD pattern with that from THF-H_2O solution.*

* A referee suggested the possibility that the precipitate of the short rod-like structure is crystallographically a chiral twin and that of the helical ribbon structure is chiral. At present, however, I have no evidence to support the possibility and thus I just mention the possibility here.

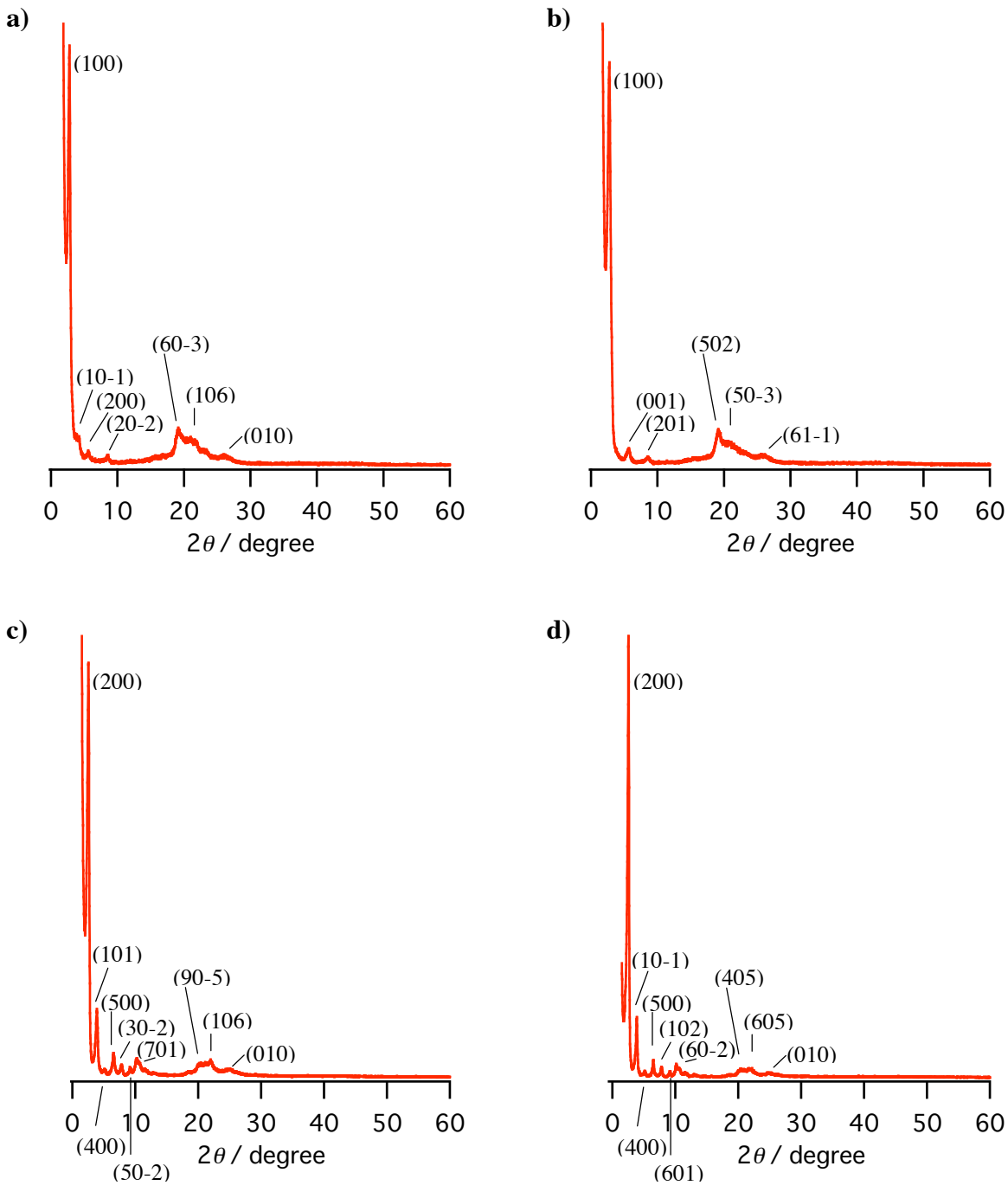

Figure 4-4. X-ray diffraction patterns of the precipitates of **1**-H_2 obtained from (a) THF-H_2O mixed solvent (1:9) and (b) a hot MeOH solution and the patterns of the precipitates of **1**-Cu obtained from (c) THF-H_2O mixed solvent (1:9) and (d) a hot MeOH solution. The XRD patterns were indexed with DASH software. The indices of the precipitates of **1**-Cu and **1**-H_2 are summarized in Table 4-1.

Table 4-1. XRD analytical data for the precipitates of **1**-H_2 and **1**-Cu.

sample	crystal system	cell parameters				
		a (Å)	*b* (Å)	*c* (Å)	β (°)	*V* (Å^3)
1-H_2 from THF-H_2O	*monoclinic*	31.43(2)	3.404(3)	25.30(2)	95.67(6)	2693
1-H_2 from hot MeOH	*monoclinic*	32.61(6)	4.455(3)	15.58(2)	98.50(7)	2239
1-Cu from THF-H_2O	*monoclinic*	67.72(6)	3.546(3)	24.61(2)	96.72(7)	5870
1-Cu from hot MeOH	*monoclinic*	68.44(3)	3.491(2)	23.44(2)	97.53(9)	5551

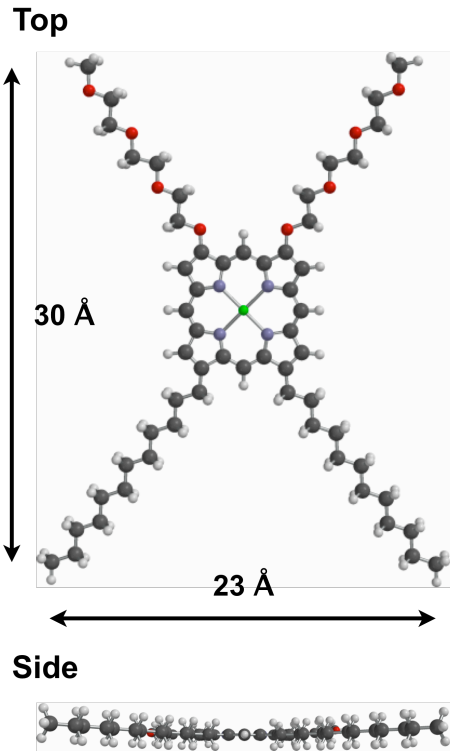

Figure 4-5. Optimized structure of **1**-Zn at AM1 level.

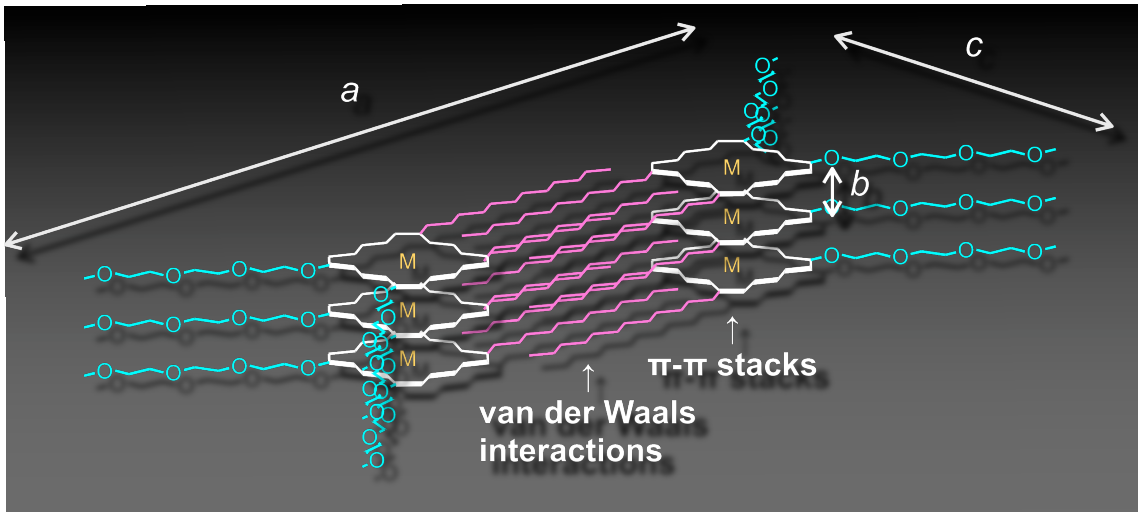

Figure 4-6. A possible structural model of the precipitates of **1**-Cu.

4-4 Thermal Magnetic Behaviors of Cu-Porphyrin Aggregates with SQUID Measurements

The thermal magnetic behaviors of **1**-Cu with SQUID measurements have been investigated in order to confirm the intermolecular metal-metal interaction induced by the supramolecular integration. The magnetic susceptibility of the precipitate obtained from THF-H_2O solution shows a bent on decreasing temperature, which indicates the weak magnetic interaction between the Cu(II) centers (Figure 4-7). The Curie-Weiss plot of the susceptibility between 4-300 K affords the Weiss constant as -0.22 K. Reflecting the same packing mode, the precipitate of **1**-Cu obtained from a hot MeOH solution shows a similar magnetic behavior with that from a THF-H_2O solution (Figure 4-8).

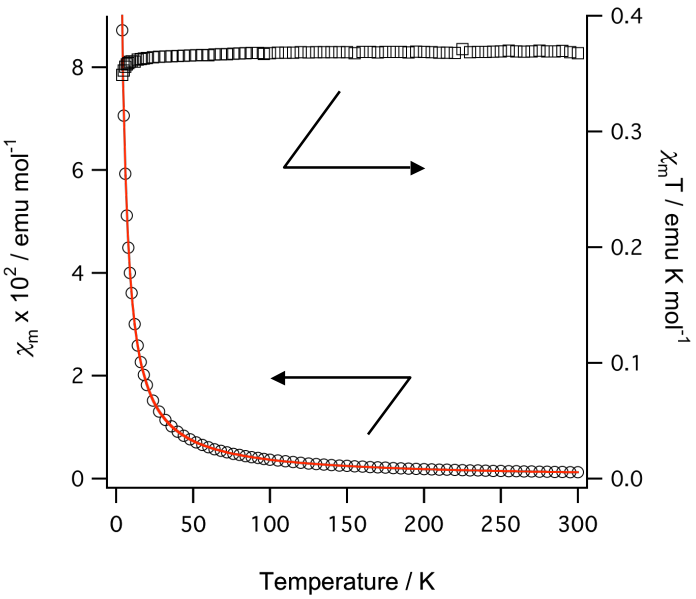

Figure 4-7. Temperature dependences of the magnetic susceptibility χ_m and $\chi_m T$ of the precipitate of **1**-Cu obtained from THF-H_2O mixed solvent. The red line express the best fit of the magnetic susceptibility χ_m to Curie-Weiss law.

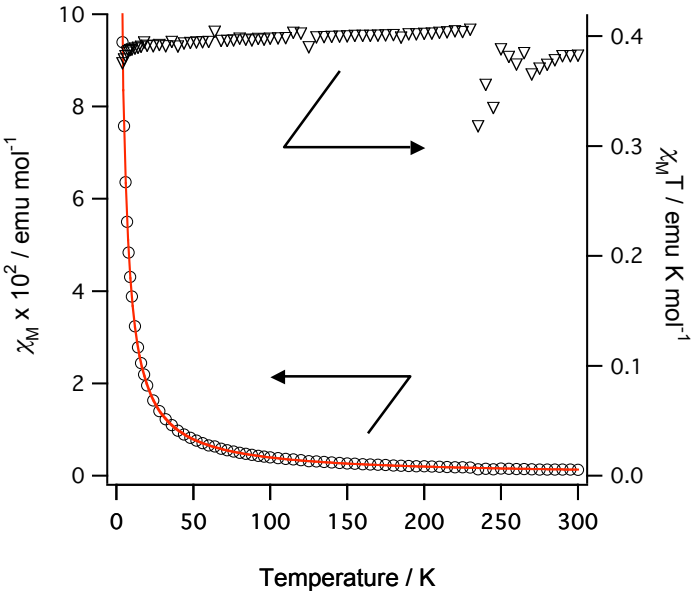

Figure 4-8. Temperature dependences of the magnetic susceptibility χ_m and $\chi_m T$ of the precipitate of **1**-Cu obtained from a hot MeOH solution. The red line expresses the best fit of the magnetic susceptibility χ_m to Curie-Weiss law.

4-5 Conclusion

I have confirmed the supramolecular integration of the porphyrin complexes under the amphiphilic conditions in polar solvents. The SEM images elucidated the morphology dependence on the precipitation solvents. In addition, the precipitates of Cu(II)-complex **1**-Cu obtained from THF-H_2O or hot MeOH solution exhibit weak magnetic interactions between the central copper atoms. The induction of intermolecular magnetic interaction between metal centers with soft-material systems is rare.

4-6 Experimental Section

General. Electronic absorption spectra were recorded on a JASCO model V–570 spectrophotometer using a quartz cell of 1–cm and 1–mm path length on equipped with a temperature controller. Field–emission scanning electron microscopy (SEM) was performed on a JEOL model JSM–6700 FE–SEM operating at an accelerating voltage of 1.5 kV. The sample was prepared by drop–casting a suspension onto HOPG substrate and then coated with carbon. Transmission Electron Microscope (TEM) images were obtained on a Hitachi model H-800 microscope in Nagoya University. The sample was prepared by drop–casting a suspension of an integrated complex onto a carbon coated copper grid. The precipitate of **1**-H_2 was stained with osmium

tetraoxide. Powder X–ray diffraction (XRD) data were recorded on a Rigaku model RINT Ultima III diffractometer by depositing the integrated precipitate on a glass substrate. The XRD analyses were carried out on DASH 3.1 for Windows (Cambridge Crystallographic Data Centre (CCDC)). The peaks were detected manually and after the calculation, the result indicating the best *Figure of Merit* value was selected for this discussion. Semi–empirical calculations at AM1 level were performed on Spartan'04 for Macintosh (Wavefunction, Inc.).

Self-assembly Processing. Self-assemblies of the porphyrins **1**-H_2 and **1**-Cu were performed through a slow diffusion of two solvents, where the molecules were transferred from a good solvent (THF) into a poor one (methanol or H_2O), which induces amphiphilic properties of the molecules to give an aggregated structure with the intermolecular π-π stacking interactions. For instance, 37.9 mg of **1**-Cu was dissolved in 7.2 mL in THF at room temperature, followed by slow addition of H_2O (65 mL). After 1 day, the solution turned to almost colorless and a red precipitate was observed at the bottom of the apparatus.

4-7 References

1. Kasha, M. *Radiat. Res.* **1963**, *20*, 55-71.

Chapter 5.

Supramolecular Integration of Porphyrins by Slow Cooling from Melting State

5-1 Advantages of Self-Assembly without Solvents

Investigations of the self-assembly in polar solvents revealed that the densely packed porphyrin supramolecules have much potentials to afford various properties dependent on the central metals (Chapter 4), because the intermolecular metal-metal interactions can be induced with these systems. This methodology, however, is not suitable for metalloporphyrins such as Zn, Fe or Mn complexes, *etc*., whose axial positions are coordinated by solvent molecules.[1] Figure 5-1 clearly shows that kind of axial coordination (methanol or THF) in zinc porphyrin **1**-Zn causes non-planar distortion of porphyrin backbone, and this sterically hindered structure cannot be densely packed in contrast to the free-base and copper porphyrin aggregates (Figure 5-2). If the amphiphilic porphyrin complexes are integrated without any solvents, many metal atoms can be utilized to the studies on metal-metal interaction in the integrated structures, and obtained metalloporphyrin aggregates might exhibit characteristic physical properties to be used for a variety of applications such as molecular magnets[2], wires of nanodevices[3] or photo-energy conversion systems[4], *etc*. One of the strategies for this purpose is supramolecular integration by slow cooling from melting state.

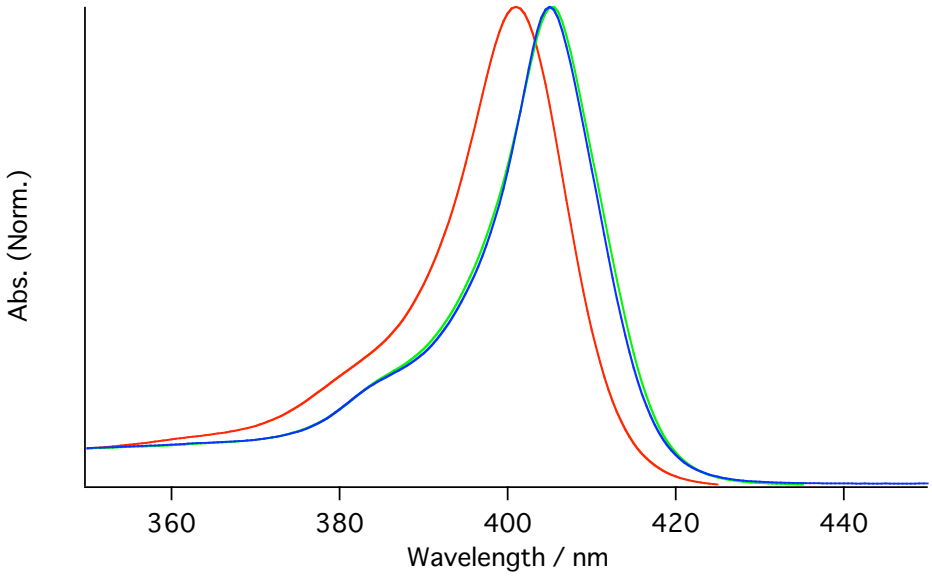

Figure 5-1. UV-Vis spectra of **1**-Zn in (red) CH_2Cl_2, (green) CH_2Cl_2-MeOH = 9:1 and (blue) THF normalized at λ_{max}.

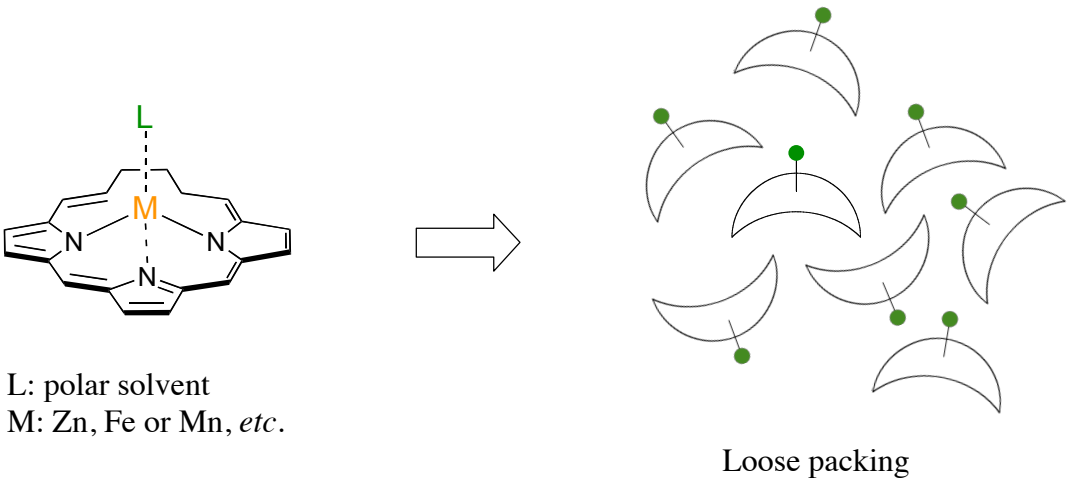

Figure 5-2. A model of the self-assembly of axially coordinated amphiphilic porphyrins in polar solvents.

5-2 DSC and POM Results of Cu-Porphyrin

Differential scanning calorimetry (DSC) measurements are powerful tools for examining phase transition behavior and thermal stability of compounds. The DSC of amorphous **1**-Cu showed two reversible transition peaks around 130 and 30 ºC (Figure 5-3). This result means that the melting point of porphyrin **1**-Cu is about 130 ºC and it is thermally stable below 300 ºC. The possibility has been investigated by polarized microscopy that a liquid-crystalline mesophase appear in temperature region between 130 and 30 ºC. But on cooling from the isotropic liquid of **1**-Cu (> 150 ºC), the resulting phase at this temperature region (POM) didn't show any dendritic textures but microcrystals (Figure 5-4(a), (b)). In addition, the second phase transition, on cooling below 30 ºC, indicated no significant changes in polarized optical micrographs (Figure 5-4(c), (d)). In conclusion, the phase transitions around 130 and 30 ºC correspond to liquid–crystal and crystal–crystal transformations, respectively. Although any liquid crystalline mesophases are not observed from porphyrin **1**-Cu, it is clearly possible to be organized by slow cooling from melting state without any solvents.

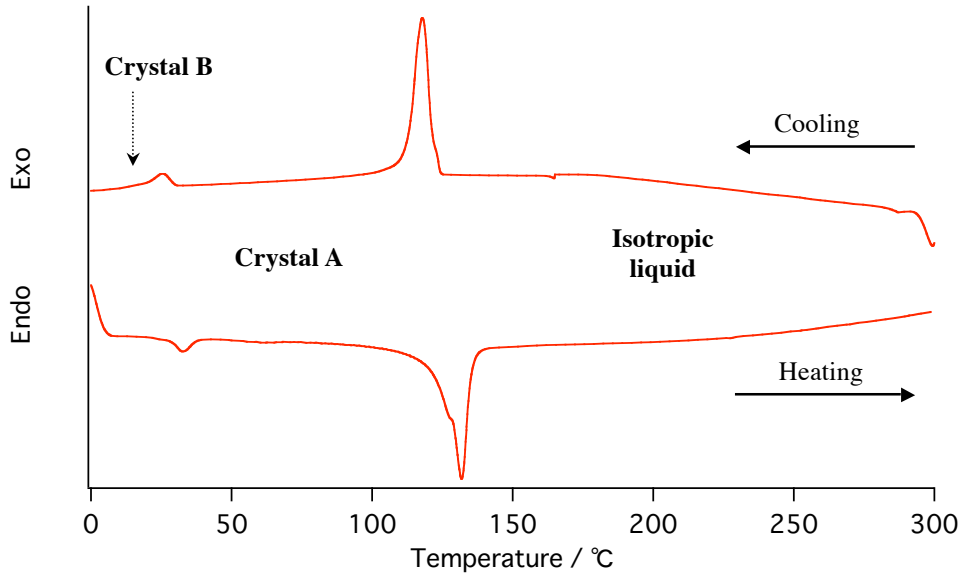

Figure 5-3. DSC traces of **1**-Cu on first cooling and second heating.

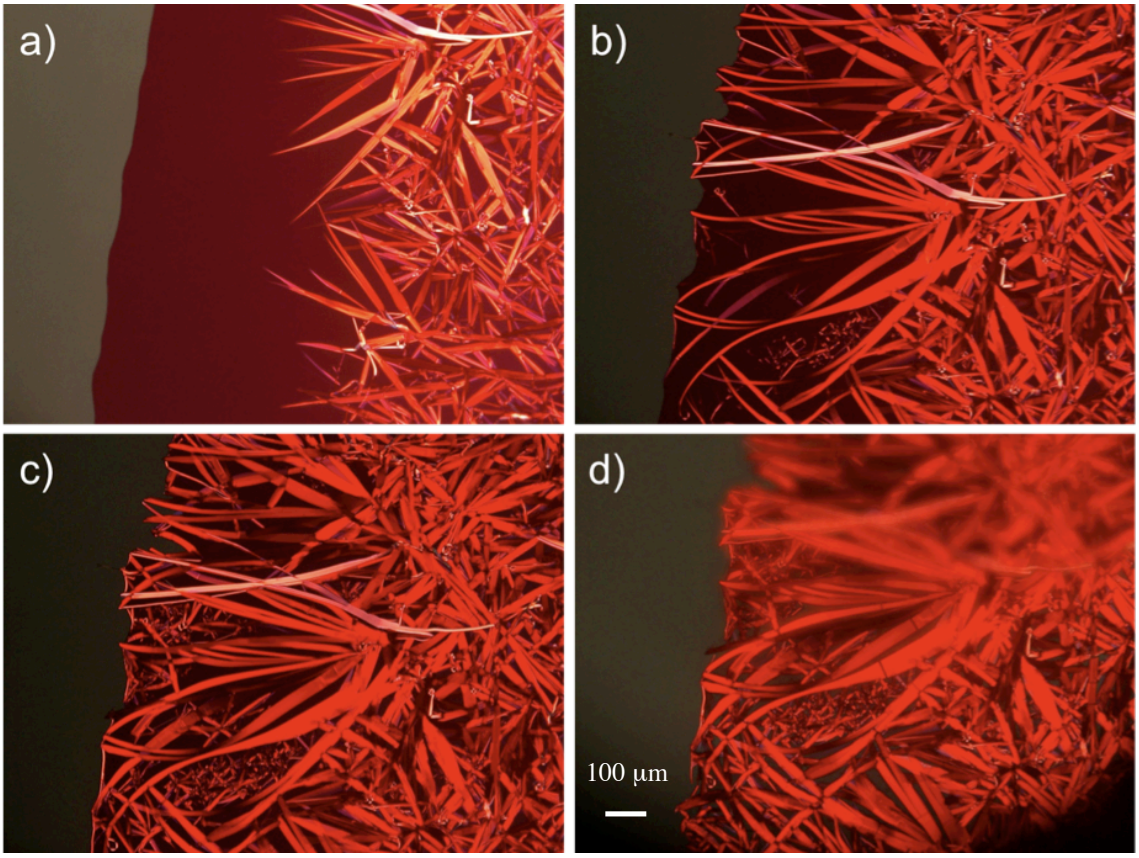

Figure 5-4. Polarized optical micrographs of **1**-Cu on cooling from 150 ℃ to (a) 130 ℃, (b) 120 ℃, (c) 30 ℃ and (d) 0 ℃.

5-3 Integration of Cu-Porphyrin into film and UV-Vis Spectroscopy

When porphyrin **1**-Cu was put between two glasses and heated in a melting-point determination apparatus, fluid-like porphyrin was observed at temperature over 130 ºC (Figure 5-5). After cooling to r. t., thin film of **1**-Cu could be obtained easily. The UV-Vis spectrum of the film showed that the λ_{max} were similar to that of **1**-Cu in THF–H_2O = 1:9 solution, but the absorption bands were more broadened (Figure 5-6). This result means that the **1**-Cu thin film might be integrated into a comparable supramolecular structure as **1**-Cu aggregates obtained from polar solvents.

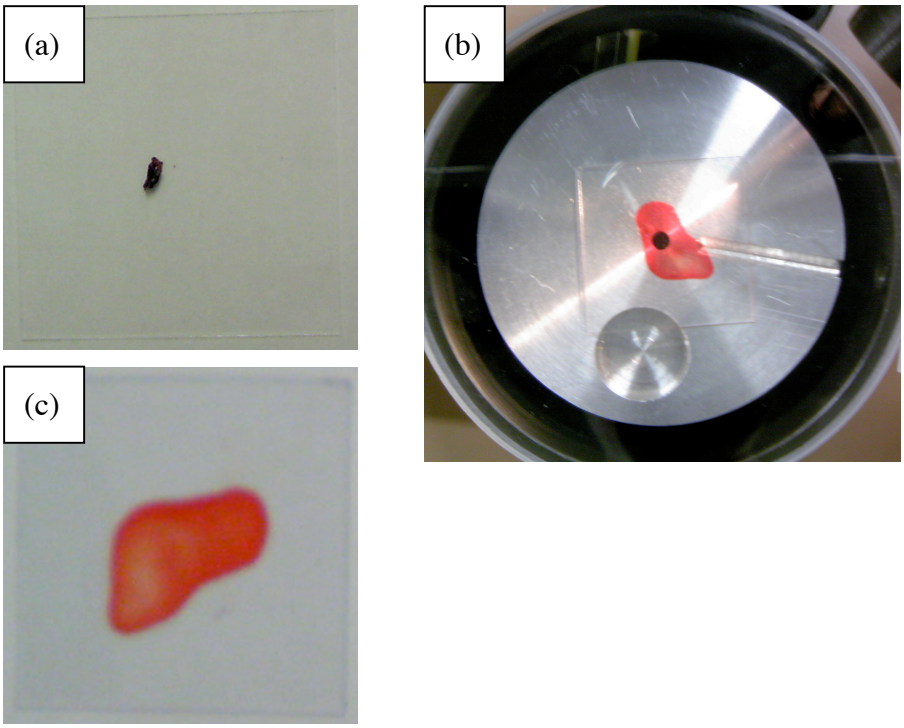

Figure 5-5. Photographs of **1**-Cu (a) before heating, (b) after melting and (c) after cooling to r. t.

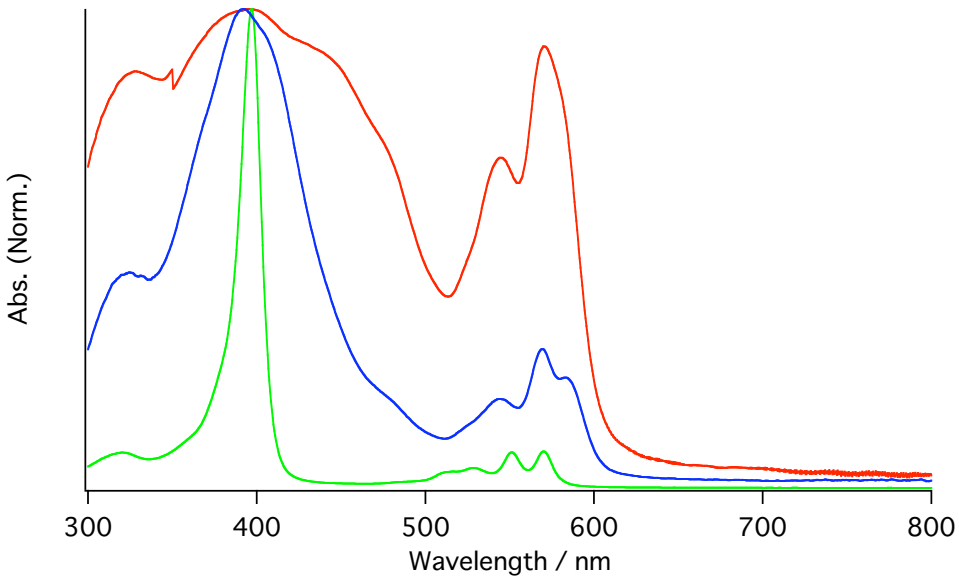

Figure 5-6. UV-Vis spectra of aggregated **1**-Cu film (red), **1**-Cu in THF-H_2O = 1:9 (blue) and in THF (green) normalized at λ_{max}.

5-4 Conclusion

The methodology has been developed to produce porphyrin aggregate from melting upon heating. From this method, thin film of **1**-Cu was obtained in short process and the porphyrin film can be investigated spectroscopically. Because of nonuse of any solvents, this procedure can be applied to supramolecular aggregations of other transition metal complexes in the same amphiphilic porphyrin.

5-5 Experimental Section

General. Electronic absorption spectra were recorded on a JASCO model V–570 spectrophotometer using a quartz cell of 1–cm and 1–mm path length on equipped with a temperature controller or glass substrates. Differential scanning calorimetry (DSC) measurements were performed on a TA Instruments TGA2950/ DSC2920/ SDT2960. Polarized optical micrographs were recorded in Tokyo Institute of Technology. Yanaco MP-S3 melting point determination apparatus was used for obtaining porphyrin film.

Film processing. Producing films of porphyrin **1**-Cu was performed on melting point determination apparatus. The amorphous solid was put into between two glasses and heated at 150 ºC, which induce the melting of porphyrin. After cooling to r. t., the red fluid turned solid again and porphyrin thin film was obtained between glass

substrates.

5-6 References

1. *The Porphyrin Handbook*, Vol. 3, Kadish, K. M.; Smith, K. M.; Guilard, R. Eds.; Academic Press; Sandiego, 2000.
2. (a) Bernot, K.; Luzon, J.; Sessoli, R.; Vindigni, A.; Thion, J.; Richeter, S.; Leclercq, D.; Larionova, J.; Lee, A. v. d. *J. Am. Chem. Soc.* **2008**, *130*, 1619-1627. (b) Caneschi, A.; Gatteschi, D.; Lalioti, N.; Sangregorio, C.; Sessoli, R.; Venturi, G.; Vindigni, A.; Rettori, A.; Pini, M. G.; Novak, M. A. *Angew. Chem. Int. Ed.* **2001**, *40*, 1760-1763. (c) Clérac, R.; Miyasaka, H.; Yamashita, M.; Coulon, C. *J. Am. Chem. Soc.* **2002**, *124*, 12837-12844.
3. (a) Mitsumi, M.; Ueda, H.; Furukawa, K.; Ozawa, Y.; Toriumi, K.; Kurmoo, M. *J. Am. Chem. Soc.* **2008**, *130*, 14102–14104. (b) Chen, L.; Kim, J.; Ishizuka, T.; Honsho, Y.; Saeki, A.; Seki, S.; Ihee, H.; Jiang, D.-L. *J. Am. Chem. Soc.* **2009**, *131*, 7287–7292. (c) Ozawa, H.; Kawao, M.; Uno, S.; Nakazato, K.; Tanaka, H.; Ogawa, T. *J. Mater. Chem.*, **2009**, *19*, 8307–8313. (d) Kobayashi, A.; Fujiwara, E.; Kobayashi, H. *Chem. Rev.* **2004**, *104*, 5243-5264.
4. Huijser, A.; Suijkerbuijk, B. M. J. M.; Gebbink, R. J. M. K.; Savenije, T. J.; Siebbeles, L. D. A. *J. Am. Chem. Soc.* **2008**, *130*, 2485-2492.

Chapter 6.

Summary and Perspectives

Novel asymmetrically β-substituted porphyrin complexes have been obtained by suppressing the scrambling problem on the condensation reaction of two dipyrromethanes. As it is difficult to synthesize lower symmetrical or complicatedly modified molecules, structural and functional studies of β-alkyl type porphyrins have not been developed rather than *meso*-aryl type one. The present methodologies can promote us to produce versatile molecular designs of β-substituted porphyrins, which have grate potentials for new porphyrin-based chemistry.

The supramoleular integration of β-substituted amphiphilic porphyrin complexes has been investigated in polar solvents or by slow cooling from melting state. Because of these highly planar and less bulky structures, the porphyrin complexes can be integrated into densely packed structures that are completely different from other reported porphyrin supramolecules. The Cu-complex of the amphiphilic porphyrin shows smaller offset H-aggregation and thus the intermolecular metal–metal distance of this aggregate is shortened enough to induce magnetic interaction. Considering other references, amphiphilicity and high planarity seem to be necessary to accomplish densely packed H-aggregation. This research is a first step of constructing 1-dimensional metal arrays with soft material system, associated with magnetic, optical or electronic properties based on intermolecular metal–metal interactions.

Abbreviation

BChl: bacteriochlorophyll

LH1, LH2: light-harvesting antenna complex 1, 2

RC: reaction center

TEG: triethyleneglycol monomethylether

DBU: 1,8-diazabicyclo[5.4.0]undec-7-ene

DMF: *N*,*N*-dimethylformamide

THF: tetrahydrofuran

TFA: trifluoroacetic acid

NMR: nuclear magnetic resonance

MALDI–TOF MS: matrix–assisted laser desorption ionization time–of–flight mass spectroscopy

FAB-MS: fast atom bombardment mass spectroscopy

HRMS: high-resolution mass spectroscopy

FT IR: Fourier transform infrared spectroscopy

UV-Vis: ultraviolet-visible light absorption spectroscopy

FE-SEM: field–emission scanning electron microscopy

TEM: transmission electron microscopy

HOPG: highly oriented pyrolytic graphite

XRD: X–ray diffraction

SQUID: superconducting quantum interference device

DSC: differential scanning calorimetry

POM: polarized optical microscopy

List of Publications and Presentations

Publications

1. Yiheng Zhang, Ying Yu, Zhenhua Jiang, Huaping Xu, Zhiqiang Wang, Xi Zhang, Masafumi Oda, Tomoya Ishizuka, Donglin Jiang, Lifeng Chi, Harald Fuchs, "Single-Molecule Study on Intermolecular Interaction between C60 and Porphyrin Derivatives: Toward Understanding the Strength of the Multivalency", *Langmuir*, **2009**, **25** (12), pp 6627–6632.

2. Masafumi Oda, Tomoya Ishizuka, Shigeo Arai, Atsushi Takano, Donglin Jiang, "Highly planar amphiphilic porphyrins", *Tetrahedron Lett*., **2009**, *50* (51), pp 7137–7140.

Presentations

(Oral)

1. ○小田　雅文、石塚　智也、江　東林、「新規両親媒性βアルキル型ポルフィリン錯体の合成と超分子組織化」、『日本化学会第 89 春季年会』、船橋、2009 年 3 月

2. ○小田　雅文、石塚　智也、江　東林、「新規両親媒性βアルキル型ポルフィリン錯体の超分子組織化の検討」、『第 58 回高分子学会年次大会』、神戸、2009

年 5 月

(Poster)

1. ○小田　雅文、石塚　智也、江　東林、「両親媒性ベータアルキル型ポルフィリン金属錯体の合成と超分子集積化」、『第 58 回錯体化学討論会』、金沢、2008 年 9 月

2. ○小田　雅文、石塚　智也、江　東林、「両親媒性βアルキル型ポルフィリンの合成とその超分子組織化」、『第 19 回基礎有機化学討論会』、吹田、2008 年 10 月

3. ○Masafumi Oda, Tomoya Ishizuka, Donglin Jiang, “Synthesis and Supramolecular Assembly of Amphiphilic β-Alkylporphyrin”, The 3rd SOKENDAI Asian Winter School, 岡崎、2008 年 12 月

4. ○Masafumi Oda, Tomoya Ishizuka, Donglin Jiang, “Supramolecular Assembly of Novel Amphiphilic *β*-Alkylporphyrin Complexes”, The Third Winter School of Asian CORE Program, 台北、2009 年 1 月

Acknowledgment

The present thesis summarizes the author's studies from 2007 to 2010 at Department of Materials Molecular Science, the Graduate University for Advanced Studies. This work is generously supported by Institute for Molecular Science and carried out under the supervision by Professor Donglin Jiang. The author wishes to express his cordial gratitude to Professor Jiang for his stimulating discussion and unfailing encouragement.

This work would not have been possible without help of Dr. Tomoya Ishizuka and the members in Division of Molecular Functions. The author is deeply indebted to Dr. Ishizuka and coworkers for continual direction and hearty encouragement. Acknowledgements are also due to Ms. Hiroko Suzuki for her office work and heartfelt kindness.

The author is really grateful to Professor Atsushi Takano and Dr. Shigeo Arai (Nagoya University) for transmission electron microscopy, Professor Kento Okoshi (Tokyo Institute of Technology) for polarized optical microscopy, and technical staffs in Institute for Molecular Science for various measurements.

The author is very appreciative of Professor Toshi Nagata and Professor Hidehiro Sakurai for meaningful suggestion and hearty sympahty.

Finally, the author expresses his sincere gratitude to his parents for their supports, generous understanding, and affectionate encouragement.

Okazaki, January 2010

Masafumi Oda